Measurements of top quark spin observables in $t\bar{t}$ events using dilepton final states in $\sqrt{s}$=8 TeV pp collisions with the ATLAS detector

EUROPEAN ORGANISATION FOR NUCLEAR RESEARCH (CERN)

JHEP 03 (2017) 113
DOI: doi:10.1007/JHEP03(2017)113

CERN-EP-2016-263
21st April 2017

Measurements of top quark spin observables in $t\bar{t}$ events using dilepton final states in $\sqrt{s} = 8$ TeV pp collisions with the ATLAS detector

The ATLAS Collaboration

Measurements of top quark spin observables in $t\bar{t}$ events are presented based on 20.2 fb^{-1} of $\sqrt{s} = 8$ TeV proton–proton collisions recorded with the ATLAS detector at the LHC. The analysis is performed in the dilepton final state, characterised by the presence of two isolated leptons (electrons or muons). There are 15 observables, each sensitive to a different coefficient of the spin density matrix of $t\bar{t}$ production, which are measured independently. Ten of these observables are measured for the first time. All of them are corrected for detector resolution and acceptance effects back to the parton and stable-particle levels. The measured values of the observables at parton level are compared to Standard Model predictions at next-to-leading order in QCD. The corrected distributions at stable-particle level are presented and the means of the distributions are compared to Monte Carlo predictions. No significant deviation from the Standard Model is observed for any observable.

Contents

1 Introduction **2**

2 ATLAS detector **3**

3 Observables **4**

4 Data and simulation samples **6**

5 Event selection and background estimation **7**
5.1 Object selection 7
5.2 Event selection 8
5.3 Background estimation 8
5.4 Kinematic reconstruction of the $t\bar{t}$ system 9
5.5 Event yields and kinematic distributions 10

6 Analysis **12**
6.1 Truth level definitions 12
6.1.1 Parton-level definition 12
6.1.2 Stable-particle definition and fiducial region 12
6.2 Unfolding 13
6.3 Systematic uncertainties 14
6.3.1 Detector modelling uncertainties 17
6.3.2 Background-related uncertainties 18
6.3.3 Modelling uncertainties 18
6.3.4 Other uncertainties 19

7 Results **20**

8 Conclusion **27**

1 Introduction

The top quark, discovered in 1995 by the CDF and D0 experiments at the Tevatron at Fermilab [1, 2], is the heaviest fundamental particle observed so far. Its mass is of the order of the electroweak scale, which suggests that it might play a special role in electroweak symmetry breaking. Furthermore, since the top quark has a very short lifetime of $O(10^{-25}$ s) [3–5] it decays before hadronisation and before any consequent spin-flip can take place. This offers a unique opportunity to study the properties of a bare quark and, in particular, the properties of its spin.

Top quarks at the LHC are mostly produced in $t\bar{t}$ pairs via the strong interaction, which conserves parity. The quarks[1] and gluons of the initial state are unpolarised, which means that their spins are not preferentially aligned with any given direction. The top quarks produced in pairs are thus unpolarised except for the contribution of weak corrections and QCD absorptive parts at the per-mill level [6]. However, the spins of the top and antitop quarks are correlated with a strength depending on the spin quantisation

[1] Antiparticles are generally included in the discussions unless otherwise stated.

axis and on the production process. Various new physics phenomena can alter the polarisation and spin correlation due to alternative production mechanisms [6–9]. The spins of the top quarks do not become decorrelated due to hadronisation, and so their spin information is transferred to their decay products. This makes it possible to measure the top quark pair's spin structure using angular observables of their decay products. The predictions for many of these observables are available at next-to-leading order (NLO) in quantum chromodynamics (QCD). A few of them have been measured by the experiments at the LHC and Tevatron and found to be in good agreement with the Standard Model (SM) predictions [10–18].

This paper presents the measurement of a set of 15 spin observables with a data set corresponding to an integrated luminosity of 20.2 fb^{-1} of proton–proton collisions at $\sqrt{s} = 8$ TeV, recorded by the ATLAS detector at the LHC in 2012. Each of the 15 observables is sensitive to a different coefficient of the top quark pair's spin density matrix, probing different symmetries in the production mechanism [19]. Ten of these observables have not been measured until now. The observables are corrected back to parton level in the full phase-space and to stable-particle level in a fiducial phase-space. At parton level, the measured values of the polarisation and spin correlation observables are presented and compared to theoretical predictions. All observables allow a direct measurement of their corresponding expectation value. At stable-particle level, the distributions corrected for detector acceptance and resolution are provided. Because of the limited phase-space used at that level, the values of the polarisation and spin correlations are not proportional to the means of these distributions. Instead, the means of the distributions are provided and compared to the values obtained in Monte Carlo simulation.

2 ATLAS detector

The ATLAS detector [20] at the LHC covers nearly the entire solid angle around the interaction point.[2] It consists of an inner tracking detector surrounded by a thin superconducting solenoid, electromagnetic and hadronic calorimeters, and a muon spectrometer incorporating superconducting toroid magnets.

The inner-detector system is immersed in a 2 T axial magnetic field and provides charged-particle tracking in the pseudorapidity range $|\eta| < 2.5$. A high-granularity silicon pixel detector covers the interaction region and typically provided three measurements per track in 2012. It is surrounded by a silicon microstrip tracker designed to provide eight two-dimensional measurement points per track. These silicon detectors are complemented by a transition radiation tracker, which enables radially extended track reconstruction up to $|\eta| = 2.0$. The transition radiation tracker also provides electron identification information based on the fraction of hits (typically 30 in total) exceeding an energy-deposit threshold consistent with transition radiation.

The calorimeter system covers the pseudorapidity range $|\eta| < 4.9$. Within the region $|\eta| < 3.2$, electromagnetic calorimetry is provided by barrel and endcap high-granularity lead/liquid-argon (LAr) electromagnetic calorimeters, with an additional thin LAr presampler covering $|\eta| < 1.8$ to correct for energy loss in the material upstream of the calorimeters. Hadronic calorimetry is provided by a steel/scintillator-tile calorimeter, segmented into three barrel structures within $|\eta| < 1.7$, and two copper/LAr hadronic endcap calorimeters. The solid angle coverage is completed with forward copper/LAr and tungsten/LAr calorimeters used for electromagnetic and hadronic measurements, respectively.

[2] ATLAS uses a right-handed coordinate system with its origin at the nominal interaction point (IP) in the centre of the detector and the z-axis along the beam pipe. The x-axis points from the IP to the centre of the LHC ring, and the y-axis points upward. Cylindrical coordinates (r, ϕ) are used in the transverse plane, ϕ being the azimuthal angle around the beam pipe. The pseudorapidity is defined in terms of the polar angle θ as $\eta = -\ln[\tan(\theta/2)]$.

The muon spectrometer comprises separate trigger and high-precision tracking chambers measuring the deflection of muons in a magnetic field generated by superconducting air-core toroids. The precision chamber system covers the region $|\eta| < 2.7$ with drift tube chambers, complemented by cathode strip chambers. The muon trigger system covers the range $|\eta| < 1.05$ with resistive plate chambers, and the range $1.05 < |\eta| < 2.4$ with thin gap chambers.

A three-level trigger system is used to select interesting events. The Level-1 trigger is implemented in hardware and uses a subset of detector information to reduce the event rate to a design value of at most 75 kHz. This is followed by two software-based trigger levels, which together reduce the event rate to about 400 Hz.

3 Observables

The spin information of the top quarks, encoded in the spin density matrix, is transferred to their decay particles and affects their angular distributions. The spin density matrix can be expressed by a set of several coefficients: one spin-independent coefficient, which determines the cross section and which is not measured here, three polarisation coefficients for the top quark, three polarisation coefficients for the antitop quark, and nine spin correlation coefficients. By measuring a set of 15 polarisation and spin correlation observables, the coefficient functions of the squared matrix element can be probed. The approach used in this paper was proposed in Ref. [19]. The normalised double-differential cross section for $t\bar{t}$ production and decay is of the form [6, 21]

$$\frac{1}{\sigma}\frac{\mathrm{d}^2\sigma}{\mathrm{d}\cos\theta^a_+\,\mathrm{d}\cos\theta^b_-} = \frac{1}{4}(1 + B^a_+\cos\theta^a_+ + B^b_-\cos\theta^b_- - C(a,b)\cos\theta^a_+\cos\theta^b_-), \tag{1}$$

where B^a, B^b and $C(a,b)$ are the polarisations and spin correlation along the spin quantisation axes a and b. The angles θ^a and θ^b are defined as the angles between the momentum direction of a top quark decay particle in its parent top quark's rest frame and the axis a or b. The subscript $+(-)$ refers to the top (antitop) quark. From Equation (1) one can retrieve the following relation for the spin correlation between the axes a and b

$$C(a,b) = -9 < \cos\theta^a_+\cos\theta^b_- > . \tag{2}$$

Integrating out one of the angles in Equation (1) gives the single-differential cross section

$$\frac{1}{\sigma}\frac{\mathrm{d}\sigma}{\mathrm{d}\cos\theta^a} = \frac{1}{2}(1 + B^a\cos\theta^a). \tag{3}$$

This means the differential cross section has a linear dependence on the polarisation B^a, from which also follows

$$B^a = 3 < \cos\theta^a > . \tag{4}$$

All the observables are based on $\cos\theta$, which is defined using three orthogonal spin quantisation axes:

- The helicity axis is defined as the top quark direction in the $t\bar{t}$ rest frame. In Ref. [19] it is indicated by the letter k, a notation which is adopted in this paper. Measurements of the polarisation and spin correlation defined along this axis at 7 and 8 TeV were consistent with the SM predictions [10–16].

Expectation values	NLO predictions	Observables
B^k_+	0.0030 ± 0.0010	$\cos\theta^k_+$
B^k_-	0.0034 ± 0.0010	$\cos\theta^k_-$
B^n_+	0.0035 ± 0.0004	$\cos\theta^n_+$
B^n_-	0.0035 ± 0.0004	$\cos\theta^n_-$
B^r_+	0.0013 ± 0.0010	$\cos\theta^r_+$
B^r_-	0.0015 ± 0.0010	$\cos\theta^r_-$
$C(k,k)$	0.318 ± 0.003	$\cos\theta^k_+ \cos\theta^k_-$
$C(n,n)$	0.332 ± 0.002	$\cos\theta^n_+ \cos\theta^n_-$
$C(r,r)$	0.055 ± 0.009	$\cos\theta^r_+ \cos\theta^r_-$
$C(n,k) + C(k,n)$	0.0023	$\cos\theta^n_+ \cos\theta^k_- + \cos\theta^k_+ \cos\theta^n_-$
$C(n,k) - C(k,n)$	0	$\cos\theta^n_+ \cos\theta^k_- - \cos\theta^k_+ \cos\theta^n_-$
$C(n,r) + C(r,n)$	0.0010	$\cos\theta^n_+ \cos\theta^r_- + \cos\theta^r_+ \cos\theta^n_-$
$C(n,r) - C(r,n)$	0	$\cos\theta^n_+ \cos\theta^r_- - \cos\theta^r_+ \cos\theta^n_-$
$C(r,k) + C(k,r)$	-0.226 ± 0.004	$\cos\theta^r_+ \cos\theta^k_- + \cos\theta^k_+ \cos\theta^r_-$
$C(r,k) - C(k,r)$	0	$\cos\theta^r_+ \cos\theta^k_- - \cos\theta^k_+ \cos\theta^r_-$

Table 1: List of the observables and corresponding expectation values measured in this analysis. The SM predictions at NLO are also shown [19]; expectation values predicted to be 0 at NLO are exactly 0 due to term cancellations. The expectation values can be obtained from the corresponding observables using the relations from Equations (2) and (4). The uncertainties on the predictions refer to scale uncertainties only; values below 10^{-4} are not quoted.

- The transverse axis is defined to be transverse to the production plane [6, 22] created by the top quark direction and the beam axis. It is denoted by the letter n. The polarisation along that axis was measured by the D0 experiment [17].
- The r-axis is an axis orthogonal to the other two axes, denoted by the letter r. No observable related to this axis has been measured previously.

As the dominant initial state of $t\bar{t}$ production at the LHC (gluon–gluon fusion) is Bose-symmetric, $\cos\theta$ calculations with respect to the transverse or r-axis are multiplied by the sign of the scattering angle $y = \hat{\mathbf{p}} \cdot \hat{\mathbf{k}}$, where $\hat{\mathbf{k}}$ is the top quark direction in the $t\bar{t}$ rest frame and $\hat{\mathbf{p}} = (0, 0, 1)$, as recommended in Ref. [19]. In the calculations of $\cos\theta$ with respect to the negatively charged lepton, the axes are multiplied by -1. The observables and corresponding expectation values, as well as their SM predictions at NLO, are shown in Table 1. The first six observables correspond to the polarisations of the top and antitop quarks along the various axes, the other nine to the spin correlations. In order to distinguish between the correlation observables, the correlations using only one axis are referred to as spin correlations and the last six as cross correlations. The predictions are computed for a top quark mass of 173.34 GeV [23]. In order to measure all observables, the final-state particles of both decay chains must be reconstructed and correctly identified. As charged leptons retain more information about the spin state of the top quarks, and as they can be precisely reconstructed, the measurement in this paper is performed in the dileptonic final state of $t\bar{t}$ events. The charged leptons considered in this analysis are electrons or muons, either originating directly from W and Z decays, or through an intermediate τ decay.

Process	Generator	Parton shower	PDF set	Tune
$t\bar{t}$	Powheg-hvq [36]	Pythia6	CT10 [30]	Perugia2011C [32]
Single top (Wt-channel)	Powheg-hvq	Pythia6	CT10	Perugia2011C
Drell–Yan	Alpgen	Pythia6	CTEQ6L1 [37]	Perugia2011C
Dibosons (WW,WZ,ZZ)	Alpgen	Herwig6+Jimmy	CTEQ6L1	AUET2 [38]
$t\bar{t}V$ ($V = W/Z/\gamma^*$)	MadGraph	Pythia8	CTEQ6L1	AUET2B
Single top, t-channel	AcerMC	Pythia6	CTEQ6L1	Perugia2011C
W+jets	Alpgen	Pythia6	CTEQ6L1	Perugia2011C
$W+\gamma$+jets	Alpgen	Herwig6+Jimmy	CTEQ6L1	AUET2

Table 2: MC generators and parton showers used for the signal and background processes. Samples in the lower part of the table are used together with the other samples to estimate the fake-lepton background. The parton distribution functions (PDF) used by the generator and the tunes used for the parton shower are also shown. The versions of the different generators are 2.14 for Alpgen [39], 5.1.4.8 for MadGraph [40], 4.31 for Herwig6+Jimmy [41], 1, r2330 for Powheg-hvq, 6.426 for Pythia6 [31] and 8.165 for Pythia8 [42].

4 Data and simulation samples

The analysis is performed using the full 2012 proton–proton collision data sample at $\sqrt{s} = 8$ TeV recorded by the ATLAS detector. The data sample corresponds to an integrated luminosity of 20.2 fb^{-1} after requiring stable LHC beams and a fully operational detector.

The analysis uses Monte Carlo (MC) simulations, in particular to estimate the sample composition and to correct the measurement to both parton and stable-particle level. The nominal $t\bar{t}$ signal MC sample is generated by Powheg-hvq (version 1, r2330) [24–27] with the top quark mass set to 172.5 GeV and the h_{damp} parameter[3] set to the top quark mass. The PDF set used is CT10 [30]. The signal events are then showered with Pythia6 (version 6.426) [31] using a set of tuned parameters named the Perugia2011C tune [32]. The background processes are also modelled using a range of MC generators which are listed in Table 2. An additional background originating from non-prompt and misreconstructed (called "fake") leptons is also estimated from MC simulation. To estimate this background, all samples listed in Table 2 are used, and in particular those listed in the lower part of the table, which are generated specifically for that background. Multijet events are not included in this list because the probability of having two jets misidentified as isolated leptons is very small. The contribution from these events is thus negligible.

In order to account for systematic uncertainties in the signal modelling, different MC samples, documented in Table 3, are compared with each other as described in Section 6.3.3.

The nominal signal and background samples were processed through a simulation of the detector geometry and response [33] using Geant4 [34]. MC samples used to estimate signal modelling uncertainties were processed with the ATLFAST-II [35] simulation. This employs a parameterisation of the response of the electromagnetic and hadronic calorimeters, and uses Geant4 for the other detector components.

[3] The h_{damp} parameter controls the hardness of the hardest emission which recoils against the $t\bar{t}$ system [28, 29].

Systematic uncertainty	Generator	Parton shower	Tune
Colour reconnection	POWHEG-hvq	PYTHIA6	Perugia2012 [32] Perugia2012loCR
Underlying event	POWHEG-hvq	PYTHIA6	Perugia2012 Perugia2012mpiHi
Parton shower	POWHEG-hvq	PYTHIA6 HERWIG	Perugia2011C AUET2
Generator	POWHEG-hvq MC@NLO	HERWIG	AUET2
ISR/FSR	POWHEG-hvq	PYTHIA6	Perugia2012radLo Perugia2012radHi
Top-quark mass	POWHEG-hvq	PYTHIA6	Perugia2011C with various mass points

Table 3: List of $t\bar{t}$ samples used for studies of the modelling uncertainties. The PDF set is CT10 for all of them. The version of the MC@NLO generator [43, 44] is 4.01.

5 Event selection and background estimation

Reconstructed objects such as electrons, muons or jets are built from the detector information and used to form a $t\bar{t}$-enriched sample by applying an event selection.

5.1 Object selection

Electron candidates are reconstructed by matching inner-detector tracks to clusters in the electromagnetic calorimeter. A requirement on the pseudorapidity of the cluster $|\eta_{\rm cl}| < 2.47$ is applied, with the transition region between barrel and endcap corresponding to $1.37 < |\eta_{\rm cl}| < 1.52$ excluded. A minimum requirement on the transverse momentum ($p_{\rm T}$) of 25 GeV is applied to match the trigger criteria (see Section 5.2). Furthermore, electron candidates are required to be isolated from additional activity in the detector. Two different criteria are used. The first one considers the activity in the electromagnetic calorimeter in a cone of size $\Delta R = 0.2$ around the electron. The second one sums the p_T of all tracks in a cone of size 0.3 around the electron track. The requirements applied on both variables are η-dependent and correspond to an efficiency on signal electrons of 90%. The final selection efficiency for the electrons used in this analysis is between 85% and 90% depending on the $p_{\rm T}$ and η of the electron [45].

Muon candidates are reconstructed by combining inner detector tracks with tracks constructed in the muon spectrometer. They are required to have a $p_{\rm T} > 25$ GeV and $|\eta| < 2.5$. They are also required to be isolated from additional activity in the inner detector. An isolation criterion requiring the scalar sum of track $p_{\rm T}$ around the muon in a cone of size $\Delta R = 10\,{\rm GeV}/p^{\mu}_{\rm T}$ to be less than $0.05 p^{\mu}_{\rm T}$ is applied. Muons have a selection efficiency of about 95% [46].

Jets are reconstructed from energy clusters in the electromagnetic and hadronic calorimeters. The reconstruction algorithm used is the anti-k_t [47] algorithm with a radius parameter of $R = 0.4$. The measured energy of the jets is corrected to the hadronic scale using $p_{\rm T}$- and η-dependent scale factors derived from simulation and validated in data [48]. After the energy correction, they are required to have a transverse

momentum $p_{\mathrm{T}} > 25$ GeV and a pseudorapidity $|\eta| < 2.5$. For jets with $p_{\mathrm{T}} < 50$ GeV and $|\eta| < 2.4$, the jet vertex fraction (JVF) must be greater than 0.5. The JVF is defined as the fraction of the scalar p_{T} sum of tracks associated with the jet and the primary vertex and the scalar p_{T} sum of tracks associated with the jet and any vertex. It distinguishes between jets originating from the primary vertex and jets with a large contribution from other proton interactions in the same bunch crossing (pile-up). If separated by $\Delta R < 0.2$, the jet closest to a selected electron is removed to avoid double-counting of electrons reconstructed as jets. Next, all electrons and muons separated from a jet by $\Delta R < 0.4$ are removed from the list of selected leptons to reject semileptonic decays within a jet. Jets containing b-hadrons are identified (b-tagged) by using a multivariate algorithm (MV1) [49] which uses information about the tracks and secondary vertices. If the MV1 output for a jet is larger than a predefined value, the jet is considered to be b-tagged. The value was chosen to achieve a b-tagging efficiency of 70%. With this algorithm, the probability to select a light jet (from gluons or u-, d-, s-quarks) is around 0.8%, and the probability to select a jet from a c-quark is 20%.

The missing transverse momentum $E_{\mathrm{T}}^{\mathrm{miss}}$ is defined as the magnitude of the negative vectorial sum of the transverse momenta of leptons, photons and jets, as well as energy deposits in the calorimeter not associated with any physics object [50].

5.2 Event selection

The event selection aims at maximising the fraction of $t\bar{t}$ events with a dileptonic final state. The final states are then separated according to the lepton flavours. Tau leptons are indirectly considered in the signal contribution when decaying leptonically. This leads to three different channels (ee, $\mu\mu$, $e\mu$). Different kinematic requirements have to be applied for the $e\mu$ and $ee/\mu\mu$ channels due to their different background contributions. Only events selected from dedicated electron or muon triggers are considered. The p_{T} thresholds of the triggers are 24 GeV for isolated leptons and 60 (36) GeV for single-electron (-muon) triggers without an isolation requirement. Events containing muons compatible with cosmic-ray interactions are removed. Exactly two oppositely charged electrons or muons with $p_{\mathrm{T}} > 25$ GeV are required. A requirement on the dilepton invariant mass of $m_{\ell\ell} > 15$ GeV is required in all channels. In addition, $|m_{\ell\ell} - m_Z| > 10$ GeV, where m_Z is the Z boson mass, is required in the ee and $\mu\mu$ channels to suppress the Drell–Yan background. In these channels the missing transverse momentum is required to be greater than 30 GeV. In the $e\mu$ channel, the scalar sum of the p_{T} of the jets and leptons in the event (H_{T}) is required to be $H_{\mathrm{T}} > 130$ GeV. At least two jets with at least one of them being b-tagged are required in each channel.

5.3 Background estimation

Single-top-quark and diboson backgrounds are estimated using MC simulation only. The MC estimate for the Drell–Yan and fake-lepton background is normalised using data-driven scale factors (SF). The Drell–Yan background does not contain any real $E_{\mathrm{T}}^{\mathrm{miss}}$. Non-negligible $E_{\mathrm{T}}^{\mathrm{miss}}$ can appear in a fraction of events with misreconstructed objects, which are difficult to model. Since real $E_{\mathrm{T}}^{\mathrm{miss}}$ is present in $Z \to \tau\tau$ events, no scale factors are applied to this sample. Another issue is the correct normalisation of Drell–Yan events with additional heavy-flavour (HF) jets from b- and c-quarks after the b-tagging requirement. In order to correct for these effects, three control regions are defined, from which three SF are extracted. Two correspond to the $E_{\mathrm{T}}^{\mathrm{miss}}$ modelling in $Z \to ee$ (SF_{ee}) and $Z \to \mu\mu$ events ($\mathrm{SF}_{\mu\mu}$), and one for the heavy-flavour normalisation in Z+jets events ($\mathrm{SF}_{\mathrm{HF}}$) common to the three dilepton channels. All control

regions require the same selection as the signal region with the exception that the invariant mass of the two leptons should be within 10 GeV of the Z mass. The control regions are then distinguished by dividing them into a pretag ($n_{b\text{-tag}} \geq 0$) and a b-tag region ($n_{b\text{-tag}} \geq 1$), additionally dividing the pretag region into the ee and $\mu\mu$ channels. The purity of the pretag control region is 97% on average for both channels. The purity of the b-tag region is 75%. The SF are extracted by solving a system of equations which relates the number of events in data and in simulation in the three control regions. The lepton-flavour-dependent scale factors $\mathrm{SF}_{ee/\mu\mu}$ are 0.927 ± 0.005 and 0.890 ± 0.004 respectively for the ee and $\mu\mu$ channels while the heavy-flavour scale factor $\mathrm{SF}_{\mathrm{HF}}$ is 1.70 ± 0.03, where the uncertainties are only statistical.

The shape of the fake and non-prompt lepton background distributions are taken from MC simulation but the normalisation is derived from data in a control region enriched in fake leptons. This is achieved by applying the same requirements as for the signal region, except that two leptons of the same charge are required. As fake leptons have approximately the same probability of having negative or positive charge, the same number of fake-lepton events should populate the opposite-sign and same-sign selection regions. The same-sign control region has a smaller background contribution from other processes, allowing the study of the modelling of the fake-lepton background. Channel-dependent scale factors are derived by normalising the predictions to data in the control regions, while the shapes of the distributions are taken from MC simulation. The SF in the ee and $e\mu$ channels are around 1.0 and 1.5, whereas the SF in the $\mu\mu$ channel is about 4. The differences between the three scale factors originate from the sources of misidentified electrons and muons, which seem to be modelled better in MC simulation for the electrons. However, the shapes of the distributions of several kinematic variables in the $\mu\mu$ channel are cross-checked in control regions and found to be consistent with the distributions from a purely data-driven method. The relative statistical uncertainties are about 20% in the same-flavour channels and 10% in the $e\mu$ channel.

5.4 Kinematic reconstruction of the $t\bar{t}$ system

The dileptonic $t\bar{t}$ final state consists of two charged leptons, two neutrinos and at least two jets originating from the top quark decay. As the neutrinos cannot be directly observed in the detector, the kinematics of the $t\bar{t}$ system, which is necessary to construct the observables, cannot be simply reconstructed from the measured information. To solve the kinematic equations and reconstruct the $t\bar{t}$ system, the neutrino weighting technique [51, 52] is used.

As input, the method uses the measured lepton and jet momenta. The masses of the top quarks are set to their generated mass of 172.5 GeV whereas the masses of the W bosons are set to their PDG values [53] in the calculations. A hypothesis is made for the value of the pseudorapidity of each neutrino and the kinematics of the system is then solved. For each solution found, a weight is assigned to quantify the level of agreement between the vectorial sum of neutrino transverse momenta and the measured $E_{\mathrm{T}}^{\mathrm{miss}}$ components. The pseudorapidities of the neutrinos are scanned independently between -5 and 5 with fixed steps of 0.025 in the range $[-2, 2]$ and of 0.05 outside of that range. All possible combinations of jets and leptons are tested. Additionally, the resolution of the jet energy measurement is taken into account by smearing the energy of each jet 50 times. The smearing is done using transfer functions mapping the energy at particle level to the energy after detector simulation. Out of all the solutions obtained, the one with the highest weight is selected. The reconstruction efficiency of the kinematic reconstruction in the $t\bar{t}$ signal sample is about 88%. No solution is found for the remaining events.

5.5 Event yields and kinematic distributions

Figure 1 shows the jet multiplicity, lepton p_{T} and jet p_{T} for all three channels. Figure 2 shows kinematic distributions of the top quark and the $t\bar{t}$ system after the event reconstruction. The data are well modelled by the MC predictions. The corrections to the Drell–Yan and fake-lepton backgrounds are applied. Only the events passing the kinematic reconstruction are considered in the distributions. The total number of predicted events is slightly lower than the number of observed events, but the two are compatible within the systematic uncertainties. The measurement is insensitive to a difference of normalisation of the signal. There is also a slight slope in the ratio between data and prediction for the lepton and top quark p_{T} distributions. This is related to a known issue in the modelling of the top quark p_{T}, described in Section 6.3.3.

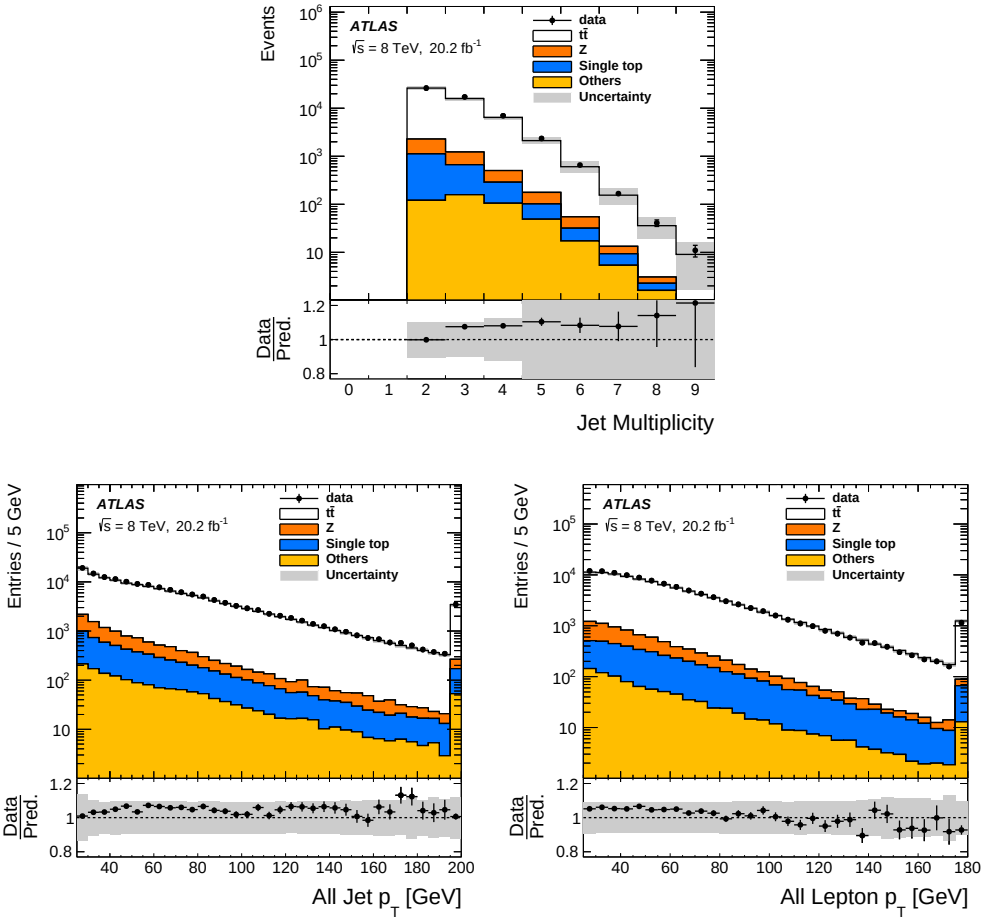

Figure 1: Comparison of the number of jets, jet p_{T} and lepton p_{T} distributions between data and predictions after the event selection in the combined dilepton channel. The ratio between the data and prediction is also shown. The grey area shows the statistical and systematic uncertainty on the signal and background. The $t\bar{t}V$, diboson and fake-lepton backgrounds are shown together in the "Others" category. Only the events passing the kinematic reconstruction are considered in the distributions.

The final yields for each channel as well as for the inclusive channel combining ee, $e\mu$ and $\mu\mu$, along with their combined statistical and systematic uncertainties, can be found in Table 4. The predictions agree

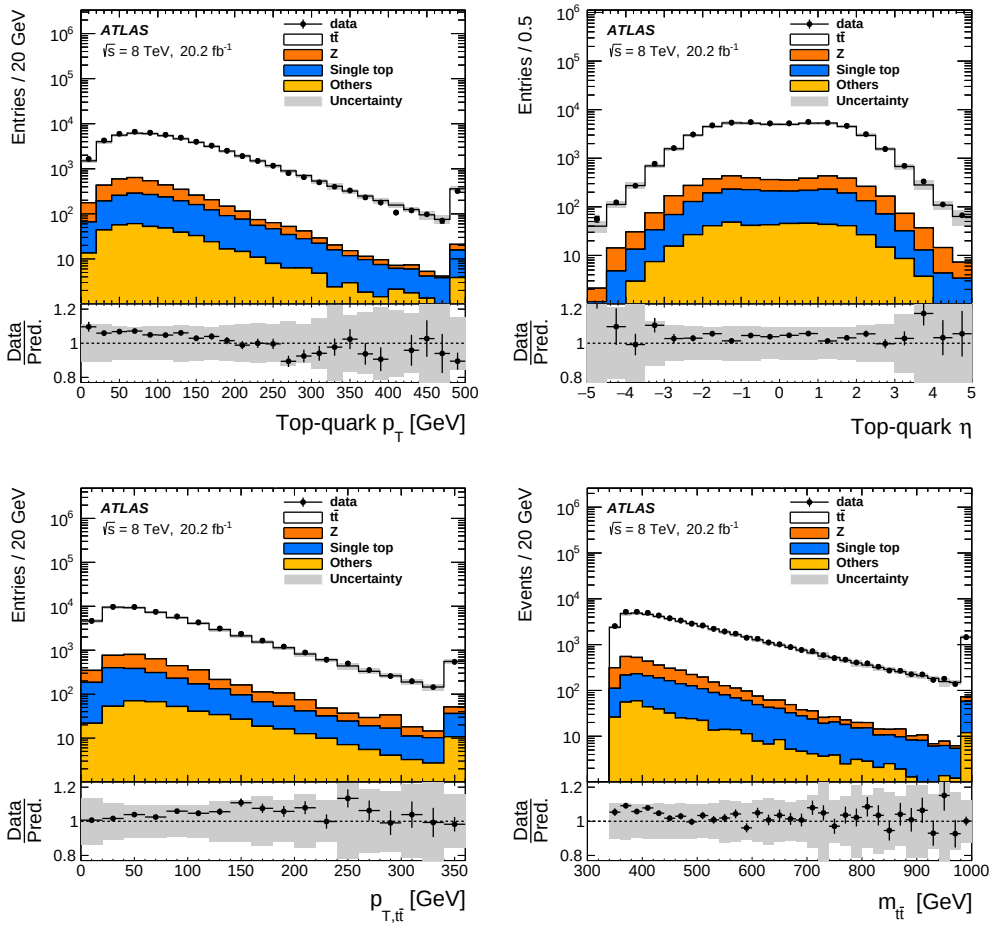

Figure 2: Comparison between data and predictions after the kinematic reconstruction in the combined dilepton channel. The distributions of the top quark p_{T} and η are shown, as well as the $t\bar{t}$ p_{T} and mass. The ratio between the data and prediction is also shown. The grey area shows the statistical and systematic uncertainty on the signal and background. The $t\bar{t}V$, diboson and fake-lepton backgrounds are shown together in the "Others" category. The last bin of the distribution corresponds to the overflow.

Channel	ee	$e\mu$	$\mu\mu$	$\ell\ell$
$t\bar{t}$	9140 ± 730	27400 ± 1900	10800 ± 710	47340 ± 2160
Fakes	47 ± 78	126 ± 62	42 ± 32	215 ± 105
Single-top	342 ± 34	1024 ± 85	396 ± 35	1762 ± 98
Diboson	17 ± 4	47 ± 7	25 ± 4	89 ± 9
$t\bar{t}V$	32 ± 35	82 ± 85	35 ± 38	149 ± 99
$Z \to ee$	910 ± 200	–	–	910 ± 200
$Z \to \mu\mu$	–	–	1100 ± 230	1100 ± 230
$Z \to \tau\tau$	25 ± 10	93 ± 20	46 ± 15	164 ± 27
Total Expected	10510 ± 760	28800 ± 1900	12460 ± 750	51750 ± 2180
Data	11162	29985	12430	53577

Table 4: Event yields of $t\bar{t}$ signal, background processes and data after the full event selection and the kinematic reconstruction. The given uncertainties correspond to the combination of statistical and systematic uncertainties of the individual processes. The last column represents the inclusive dilepton channel.

with data within uncertainties in all channels.

6 Analysis

Two different measurements of the spin observables are performed. One set of measurements is corrected to parton level and the other set is corrected to stable-particle level. These two levels are defined in the next section, as well as the phase-spaces to which the measurements are corrected.

6.1 Truth level definitions

6.1.1 Parton-level definition

At parton level, the considered top quarks are taken from the MC history after radiation but before decay. Parton-level leptons include tau leptons before they decay into an electron or muon and before radiation. With these definitions, the polarisation can be extracted from the slope of the $\cos\theta$ distribution of parton-level particles (Equation (3)) and the correlation can be extracted from the mean value of the distribution (Equation (2)). The measurement corrected to parton level is extrapolated to the full phase-space, where all generated dilepton events are considered.

6.1.2 Stable-particle definition and fiducial region

Stable-particle level includes only particles with a lifetime larger than 30 ps. The charged leptons are required not to originate from hadrons. Photons within a cone of $\Delta R = 0.1$ around the lepton direction are considered as bremsstrahlung and so their four-momenta are added to the lepton four-momentum. Selected leptons are required to have $p_T > 25$ GeV and $|\eta| < 2.5$. Jets are clustered from all stable particles, excluding the already selected leptons, by an anti-k_t algorithm with a radius parameter $R = 0.4$.

Neutrinos can be clustered within jets. Intermediate b-hadrons have their momentum set to zero, and are allowed to be clustered into the jets along with the stable particles [54]. If after clustering a b-hadron is found in a jet, the jet is considered as b-tagged [54]. Jets must have a transverse momentum of at least 25 GeV and have a pseudorapidity of $|\eta| < 2.5$. Events are rejected if a lepton and a jet are separated by $\Delta R < 0.4$. A fiducial phase-space close to the detector and selection acceptance is defined by requiring the presence of at least two leptons and at least two jets satisfying the kinematic selection criteria. Around 32% of all generated events satisfy the fiducial requirements. No b-jet is required in the definition of the fiducial region to keep it common with other analyses not using b-tagging. The b-jets are used in the kinematic reconstruction described in the following.

The top quarks (called pseudo-top-quarks [55]) are reconstructed from the stable particles defined above. If no jets are b-tagged, the two highest-p_{T} jets are considered for the pseudo-top-quark reconstruction. Neutrinos are required not to originate from hadrons, but from W or Z decays or from intermediate tau decays. For the reconstruction, only the two neutrinos with the highest p_{T} are taken in MC events. The correct lepton–neutrino pairings are chosen as those with reconstructed masses closer to the W boson mass. The correct jet–lepton–neutrino pairings are then chosen as those with masses closer to the generated top quark mass of 172.5 GeV.

In contrast to the parton-level measurement where all events are included, events from outside the fiducial region can still pass the event selection at reconstruction level and have to be treated as additional background (called the non-fiducial background). This contribution is estimated from background-subtracted data by applying the binwise ratio of non-fiducial to total reconstructed signal events obtained from MC simulation, which is found to be constant for different levels of polarisation and correlation with an average of about 6.5%.

6.2 Unfolding

Selection requirements and detector resolution distort the reconstructed distributions. An unfolding procedure is applied to correct for these distortions. The Fully Bayesian Unfolding [56] method is used. It is based on Bayes' theorem and estimates the probability (p) of $\boldsymbol{T} \in \mathbb{R}^{N_t}$ being the true spectrum given the observed data $\boldsymbol{D} \in \mathbb{N}^{N_r}$.[4] This probability is proportional to the likelihood ($\mathcal{L}$) of obtaining the data distribution given a true spectrum and a response matrix $\mathcal{M} \in \mathbb{R}^{N_r} \times \mathbb{R}^{N_t}$. This can be expressed as

$$p\left(\boldsymbol{T}|\boldsymbol{D}, \mathcal{M}\right) \propto \mathcal{L}\left(\boldsymbol{D}|\boldsymbol{T}, \mathcal{M}\right) \cdot \pi\left(\boldsymbol{T}\right), \tag{5}$$

where π is the prior probability density for the true spectrum $\boldsymbol{T}$ and is taken to be uniform. The background is estimated as described in Section 5.3 and included in the computation of the likelihood by taking into account its contribution in data when comparing it with the true spectrum. The response matrix $\mathcal{M}$, in which each entry $\mathcal{M}_{ij}$ gives the probability of an event generated in bin i to be reconstructed in bin j, is calculated from the nominal signal sample. By taking a rectangular response matrix connecting the three different analysis channels to the same true spectrum, the channels are combined within the unfolding method. The unfolded value is taken to be the mean of the posterior distribution with its root mean square taken as the uncertainty.

[4] $\mathbb{R}$ and $\mathbb{N}$ are the sets of real and natural numbers. N_t and N_r are the number of bins for the true and reconstructed distributions.

Different systematic uncertainties are estimated within the unfolding by adding nuisance parameter terms ($\boldsymbol{\theta}$) to the likelihood for each systematic uncertainty considered. The so-called marginal likelihood is then defined as

$$\mathcal{L}(\boldsymbol{D}|\boldsymbol{T}) = \int \mathcal{L}(\boldsymbol{D}|\boldsymbol{T}, \boldsymbol{\theta}) \cdot \pi(\boldsymbol{\theta}) \mathrm{d}\boldsymbol{\theta}, \tag{6}$$

where $\pi(\boldsymbol{\theta})$ is the prior probability density for each nuisance parameter $\boldsymbol{\theta}$. They are defined as Gaussian distributions G with a mean of zero and a width of one. Systematic uncertainties can be distinguished between normalisation-changing uncertainties (θ_n) and uncertainties changing both the normalisation and the shape (θ_s) of the reconstructed distribution of signal $R(\boldsymbol{T}; \theta_s)$ and background $B(\theta_s, \theta_n)$. The marginal likelihood can then be expressed as:

$$\mathcal{L}(\boldsymbol{D}|\boldsymbol{T}) = \int \mathcal{L}(\boldsymbol{D}|R(\boldsymbol{T}; \theta_s), B(\theta_s, \theta_b)) \cdot G(\theta_s) \cdot G(\theta_b) \mathrm{d}\theta_s \mathrm{d}\theta_b. \tag{7}$$

The method is validated by performing a linearity test in which distributions with known values of the polarisation and spin correlations are unfolded. The distributions of observables are reweighted to inject different values of the polarisations and correlations. For the polarisations and spin correlations, the double-differential cross section (Equation (1)) is used, while a linear reweighting is used for the cross correlations. The unfolded value for each reweighted distribution is then compared to the true value of polarisation or spin correlation and a calibration curve is built. Non-closure in the linearity test appears as a slope different from one in the calibration curve. The number of bins and the bin widths for each observable are chosen based on its resolution and optimised by evaluating the expected statistical uncertainty and by limiting the bias in the linearity test. The binning optimisation leads to a four-bin configuration for the polarisation observables and six-bin configurations for the different correlation observables. An uncertainty is added to cover the non-closure of the linearity test, which is at most 10%. The input distribution and the response matrix normalised per true bin are shown for one example of polarisation, spin correlation, and cross correlation in Figures 3 and 4.

6.3 Systematic uncertainties

The measurement of the spin observables is affected in various ways by systematic uncertainties. Three different types of systematic uncertainties are considered: detector modelling uncertainties affecting both the signal and background, normalisation uncertainties of the background, and modelling uncertainties of the signal. The first two types are included in the marginalisation procedure. The reconstructed distribution, varied to reflect a systematic uncertainty, is compared to the nominal distribution and the average change per bin is taken as the width of the Gaussian prior, as discussed in Section 6.2. In order to estimate the impact of each source of systematic uncertainty individually, pseudodata corresponding to the sum of the nominal signal and background samples are used. The unfolding procedure with marginalisation is applied to the pseudodata and constraints on the systematic uncertainties are obtained. The strongest constraint is on the uncertainty related to the electron identification and it reduces this systematic uncertainty by 50%. The other constraints are of the order of a few percent. The constrained systematic uncertainties are then used to build the $\pm 1\sigma$ variations of the prediction. The varied pseudodata are then unfolded without marginalisation. The impact of each systematic uncertainty is computed by taking half of the difference between the results obtained from the $\pm 1\sigma$ variations of pseudodata.

Modelling systematic uncertainties for the signal process are estimated separately by building calibration curves for each sample. The unfolded value in data is calibrated to generator level using the calibration

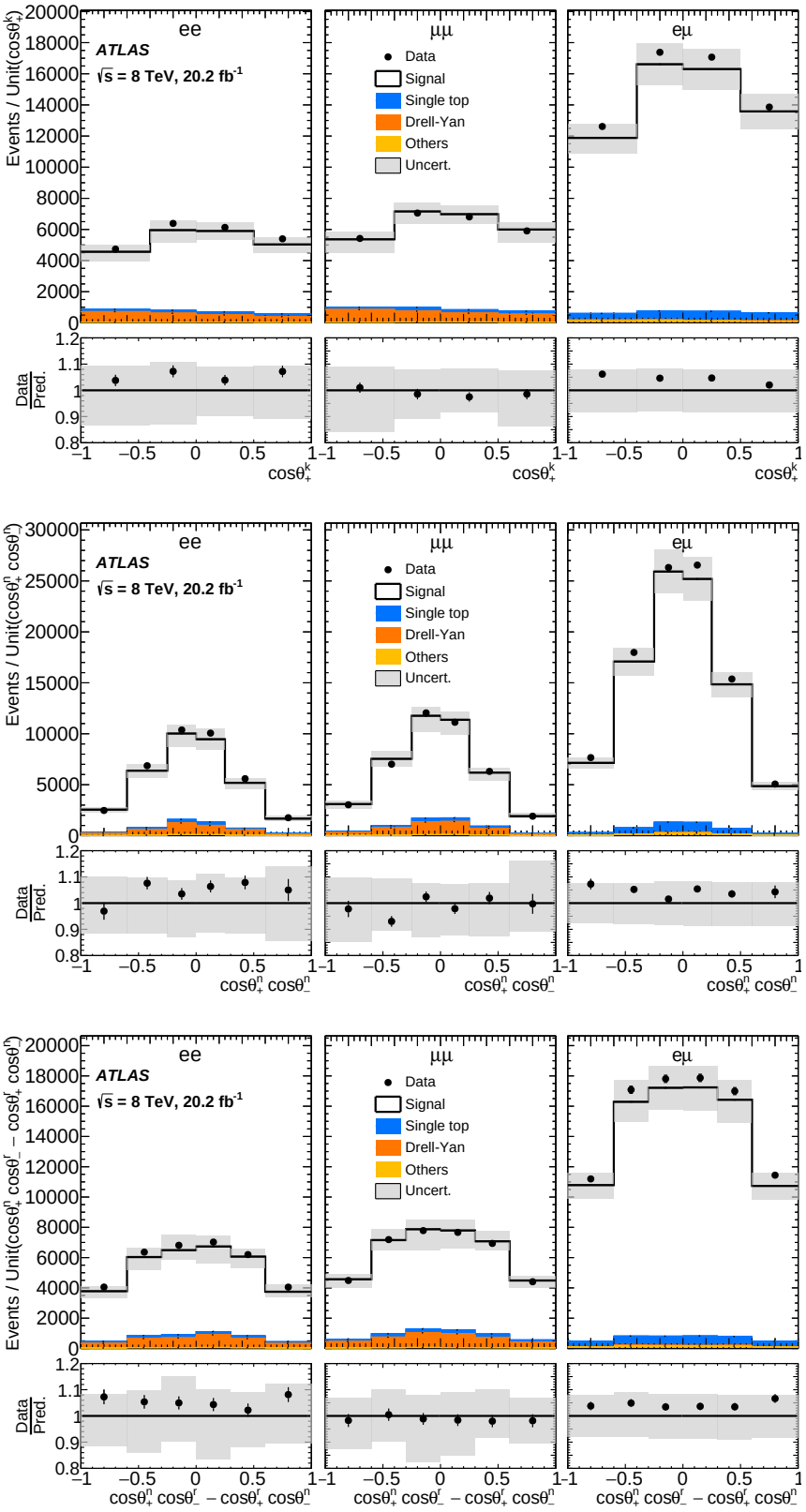

Figure 3: Input distributions for the unfolding procedure of $\cos\theta^k_+$, $\cos\theta^n_+ \cos\theta^n_-$, and $\cos\theta^n_+ \cos\theta^r_- - \cos\theta^r_+ \cos\theta^n_-$. The ratio between the data and prediction is also shown. The grey area shows the total uncertainty on the signal and background. The $t\bar{t}V$, diboson and fake-lepton backgrounds are shown together in the "Others" category.

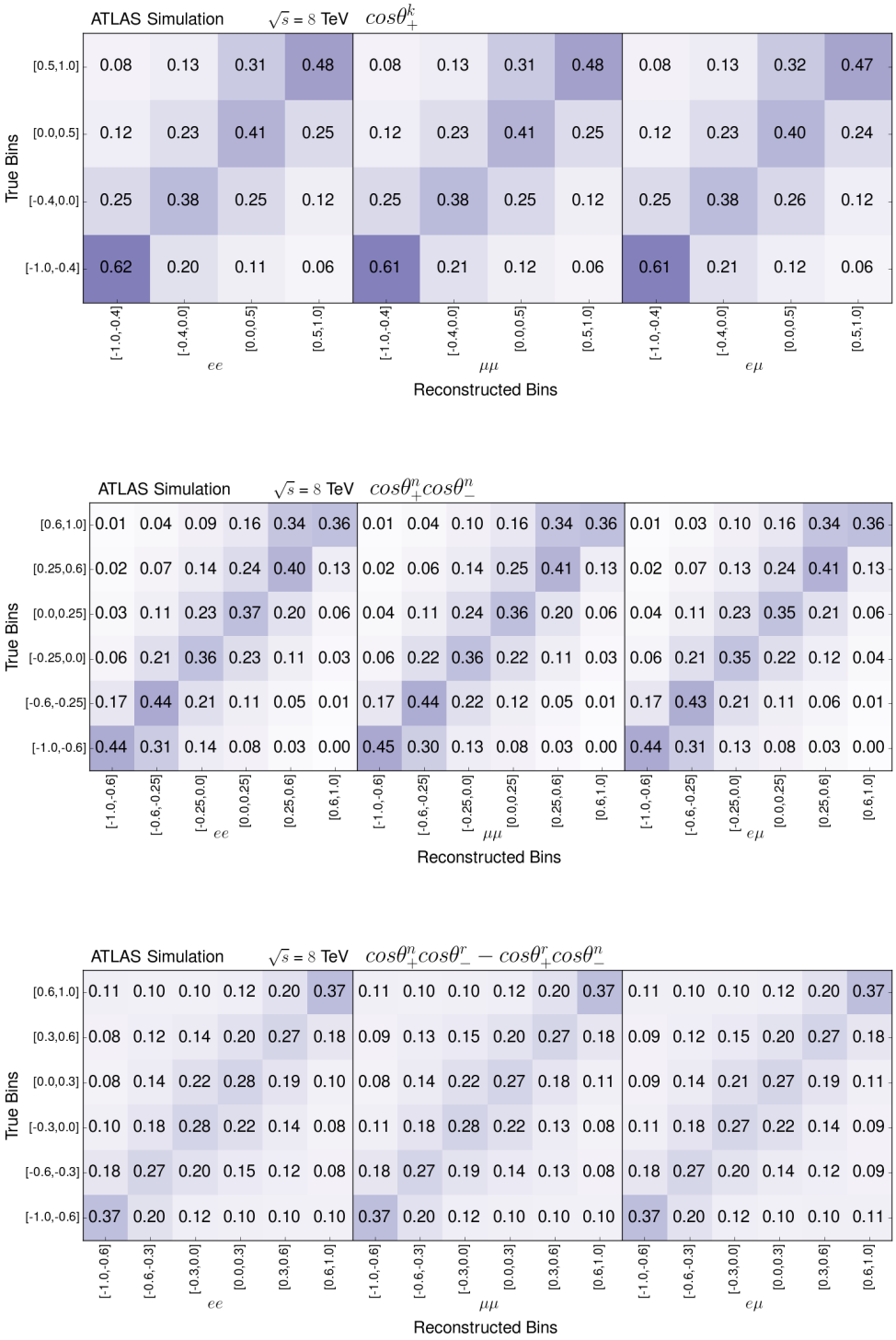

Figure 4: Response matrices of observables $\cos\theta^k_+$, $\cos\theta^n_+ \cos\theta^n_-$, and $\cos\theta^n_+ \cos\theta^r_- - \cos\theta^r_+ \cos\theta^n_-$. at parton level. They are divided into ee, $\mu\mu$, and $e\mu$ channels. The matrices are normalised per truth bin (rows) for each channel separately.

curves for the nominal sample and the sample varied to reflect the uncertainty. The difference is taken as the systematic uncertainty.

6.3.1 Detector modelling uncertainties

All sources of detector modelling uncertainty are discussed below.

Lepton-related uncertainties

- **Reconstruction, identification and trigger.** The reconstruction and identification efficiencies for electrons and muons, as well as the efficiency of the triggers used to record the events differ between data and simulation. Scale factors and their uncertainties are derived using tag-and-probe techniques on $Z \to \ell^+\ell^-(\ell = e \text{ or } \mu)$ events in data and in simulated samples to correct the simulation for these differences [57, 58].
- **Momentum scale and resolution**. The accuracy of the lepton momentum scale and resolution in simulation is checked using the $Z \to \ell^+\ell^-$ and $J/\Psi \to \ell^+\ell^-$ invariant mass distributions. In the case of electrons, E/p studies using $W \to e\nu$ events are also used. Small differences are observed between data and simulation. Corrections to the lepton energy scale and resolution, and their related uncertainties are also considered [57, 58].

Jet-related uncertainties

- **Reconstruction efficiency**. The jet reconstruction efficiency is found to be about 0.2% lower in the simulation than in data for jets below 30 GeV and it is consistent with data for higher jet p_{T}. To evaluate the systematic uncertainty due to this small inefficiency, 0.2% of the jets with p_{T} below 30 GeV are removed randomly and all jet-related kinematic variables (including the missing transverse momentum) are recomputed. The event selection is repeated using the modified number of jets.
- **Vertex fraction efficiency**. The per-jet efficiency to satisfy the jet vertex fraction requirement is measured in $Z \to \ell^+\ell^-$ + 1-jet events in data and simulation, selecting separately events enriched in hard-scatter jets and events enriched in jets from pile-up. The corresponding uncertainty is estimated by changing the nominal JVF requirement value and repeating the analysis using the modified value.
- **Energy scale**. The jet energy scale (JES) and its uncertainty were derived by combining information from test-beam data, LHC collision data and simulation [48]. The jet energy scale uncertainty is split into 22 uncorrelated sources, which have different jet p_{T} and η dependencies and are treated independently.
- **Energy resolution**. The jet energy resolution was measured separately for data and simulation. A systematic uncertainty is defined as the difference in quadrature between the jet energy resolutions for data and simulation. To estimate the corresponding systematic uncertainty, the jet energy in simulation is smeared by this residual difference.

- ***b*-tagging/mistag efficiency**. Efficiencies to tag jets from b- and c-quarks in the simulation are corrected by p_{T}- and η-dependent data/MC scale factors. The uncertainties on these scale factors are about 2% for the efficiency for b-jets, between 8% and 15% for c-jets, and between 15% and 43% for light jets [59, 60].

The dominant uncertainties in this category are related to lepton reconstruction, identification and trigger, jet energy scale and jet energy resolution. The contribution from this category to the total uncertainty is small (less than 20% for all observables).

Missing transverse momentum

The systematic uncertainties associated with the momenta and energies of reconstructed objects (leptons and jets) are propagated to the $E_{\mathrm{T}}^{\mathrm{miss}}$ calculation. The $E_{\mathrm{T}}^{\mathrm{miss}}$ reconstruction also receives contributions from the presence of low-p_{T} jets and calorimeter energy deposits not included in reconstructed objects (the "soft term"). The systematic uncertainty associated with the soft term is estimated using $Z \to \mu^+\mu^-$ events using methods similar to those used in Ref. [61]. The effect of this procedure on the measured observables is minor.

6.3.2 Background-related uncertainties

The uncertainties on the single-top-quark, $t\bar{t}V$, and diboson backgrounds are 6.8%, 10%, and 5%, respectively [62–64]. These correspond to the uncertainties on the theoretical cross sections used to normalise the MC simulated samples.

The uncertainty on the normalisation of the fake-lepton background is estimated by using various MC generators for each process contributing to this background. The scale factor in the control region is recomputed for each variation and the change is propagated to the expected number of events in the signal region. In the $\mu\mu$ channel, the uncertainty is obtained by comparing a purely data-driven method based on the measurement of the efficiencies of real and fake loose leptons, and the estimation used in this analysis. The resulting relative total uncertainties are 170% in the ee channel, 77% in the $\mu\mu$ channel and 49% in the $e\mu$ channel.

For the Drell–Yan background the detector modelling uncertainties described previously are propagated to the scale factors derived in the control region by recalculating them for all the uncertainties. An additional uncertainty of 5% is obtained by varying the control region.

Uncertainties on the shape of the different backgrounds were also estimated but found to be negligible. This category represents a minor source of uncertainty on the measurements.

6.3.3 Modelling uncertainties

These systematic uncertainties are estimated using the samples listed in Table 3.

- **Choice of MC generator.** The uncertainty is obtained by comparing samples generated with either the Powheg-hvq or the MC@NLO generator, both interfaced with Herwig. It is one of the dominant uncertainties of the measurement.

- **Parton shower and hadronisation.** This effect is estimated by comparing samples generated with POWHEG-hvq interfaced either with PYTHIA6 or HERWIG, and is one of the dominant systematic uncertainties.
- **Initial- and final-state radiations.** The uncertainty associated with the ISR/FSR modelling is estimated using POWHEG-hvq interfaced with PYTHIA6 where the parameters of the generation were varied to be compatible with the results of a measurement of $t\bar{t}$ production with a veto on additional jet activity in a central rapidity interval [65]. The difference obtained between the two samples is divided by two. This uncertainty is large and even dominant for some of the observables.
- **Colour reconnection and underlying event.** The uncertainties associated with colour reconnection and the underlying event are obtained by comparing dedicated samples with a varied colour-reconnection strength and underlying-event activity to a reference sample. All samples are generated by POWHEG-hvq and interfaced with PYTHIA6. The reference sample uses the Perugia2012 tune, the colour-reconnection sample uses the Perugia2012loCR tune, and the underlying-event sample uses the Perugia2012mpiHi tune. This uncertainty is large and even dominant for some of the observables.
- **Parton distribution functions.** PDF uncertainties are obtained by using the error sets of CT10 [30], MWST2008 [66], and NNPDF23 [67], and following the recommendations of the PDF4LHC working group [68]. The impact of this uncertainty is small.
- **Top quark p_{T} modelling.** The top quark p_{T} spectrum is not satisfactorily modelled in MC simulation [69, 70]. The impact of the mismodelling is estimated by reweighting the simulation to data and unfolding the different distributions using the nominal response matrix. The differences with respect to the nominal values are negligible compared to the other modelling uncertainties. The impact of this mismodelling is thus considered negligible, and no uncertainty is added to the total uncertainty.
- **Polarisation and spin correlation.** The response matrices used in the unfolding are calculated using the SM polarisation and spin correlation. An uncertainty related to a different polarisation and spin correlation is obtained by changing their values in the linearity test. In the reweighting procedure of the spin correlation observables, the polarisation is changed by ±0.5%, while for the polarisation observables, the spin correlation is changed by ±0.1. This uncertainty cannot be applied to the cross correlation observables as no analytic description of these observables is available. Instead, a linear reweighting is used, not depending on the polarisation or spin correlation along any axis as described in Section 6.2.

The impact of this category is large and can represent up to 85% of the total uncertainty.

6.3.4 Other uncertainties

- **Non-closure uncertainties.** When the calibration curve for the nominal signal POWHEG-hvq sample is estimated a residual slope and a non-zero offset are observed. This bias, introduced by the unfolding procedure, is propagated to the measured values. This uncertainty is small compared to the total uncertainty.

- **MC sample size.** The statistical uncertainty of the nominal signal POWHEG-hvq sample is estimated by performing pseudoexperiments on MC events. The migration matrix is varied within the MC statistical uncertainty and the unfolding procedure is repeated. The standard deviation of the unfolded polarisation or spin correlation values is taken as the uncertainty. This uncertainty is small compared to the total uncertainty.
- **Top quark mass uncertainty.** The top quark mass is assumed to be 172.5 GeV in MC simulation and in the reconstruction method. A variation of this value could have an impact on the measurement. To estimate this impact, MC samples with different values of the top quark mass are unfolded with the default response matrix. For each observable, the dependence of the unfolded value on the mass is fitted with a linear function and presented in Section 7. The slope is then multiplied by the 0.70 GeV uncertainty on the most precise ATLAS top quark mass measurements [71]. The obtained uncertainty is presented in the next section, but it is shown separately and is not included in the total uncertainty.

7 Results

Applying the unfolding procedure with marginalisation to the reconstructed distributions gives the following results at parton and stable-particle level. Table 5 presents the results for the polarisations and correlations at parton level. It shows the central value and the total uncertainty as well as a breakdown of the systematic uncertainties for the various categories described in Section 6.3. Figure 5 shows the predictions at 8 TeV calculated in Ref. [19] and the unfolded result. None of the observables deviate significantly from the SM predictions. The transverse correlation, $C(n,n)$, differs from the case of no spin correlation by 5.1 standard deviations. The correlations between the different polarisation and spin correlations were evaluated and found to be small. The highest correlations are found to be around 10% between the polarisation and spin correlation along the helicity axis and the r-axis and between some cross correlations.

Figures 6 to 8 show the observable distributions corrected back to stable-particle level and compared to the generated distribution created from POWHEG-hvq+PYTHIA6. No significant difference between the shapes of the observed and predicted distributions is observed. The means of the distributions are compared between unfolded data and MC predictions. They are presented in Table 5. In order to compare the size of the uncertainties with the parton level measurement, the means of the polarisation observables are multiplied by a factor of 3 and the correlations by a factor of -9 (Section 3). Overall the total uncertainties for the measurements at parton and particle level are comparable. The mass uncertainty is shown separately and not added to the total uncertainty, as explained in Section 6.3. The dependence of the measured polarisations and spin correlations on the MC top quark mass is presented in Table 6. The measurements presented in this paper are compatible with other direct measurements in terms of central values and uncertainties for the polarisations along the helicity and transverse axis as well as for the spin correlation along the helicity axis (Table 7).

Measurements	Central	Total	Statistical	Detector	Modelling	Others	Mass
Full phase-space							
B^k_+	−0.044	±0.038	±0.018	±0.001	±0.026	±0.007	±0.027
B^k_-	−0.064	±0.040	±0.020	±0.001	±0.023	±0.014	±0.027
B^n_+	−0.018	±0.034	±0.020	±0.001	±0.024	±0.005	-
B^n_-	0.023	±0.042	±0.020	±0.001	±0.034	±0.005	-
B^r_+	0.039	±0.042	±0.026	±0.001	±0.029	±0.005	-
B^r_-	0.033	±0.054	±0.023	±0.002	±0.045	±0.006	±0.016
$C(k,k)$	0.296	±0.093	±0.052	±0.006	±0.057	±0.011	±0.037
$C(n,n)$	0.304	±0.060	±0.028	±0.001	±0.047	±0.001	±0.010
$C(r,r)$	0.086	±0.144	±0.055	±0.005	±0.122	±0.016	±0.038
$C(n,k) + C(k,n)$	−0.012	±0.128	±0.072	±0.005	±0.087	±0.029	-
$C(n,k) - C(k,n)$	−0.040	±0.087	±0.053	±0.004	±0.058	±0.003	-
$C(n,r) + C(r,n)$	0.117	±0.132	±0.070	±0.003	±0.102	±0.010	±0.010
$C(n,r) - C(r,n)$	−0.006	±0.108	±0.069	±0.005	±0.070	±0.004	±0.043
$C(r,k) + C(k,r)$	−0.261	±0.176	±0.083	±0.006	±0.135	±0.011	±0.065
$C(r,k) - C(k,r)$	0.073	±0.192	±0.087	±0.007	±0.148	±0.005	±0.025
Fiducial phase-space							
$3\langle\cos\theta^k_+\rangle$	0.125	±0.044	±0.018	±0.007	±0.025	±0.020	±0.027
$3\langle\cos\theta^k_-\rangle$	0.119	±0.040	±0.022	±0.008	±0.021	±0.014	±0.027
$3\langle\cos\theta^n_+\rangle$	−0.025	±0.042	±0.024	±0.001	±0.027	±0.005	-
$3\langle\cos\theta^n_-\rangle$	0.023	±0.046	±0.024	±0.001	±0.036	±0.006	-
$3\langle\cos\theta^r_+\rangle$	−0.104	±0.045	±0.027	±0.008	±0.030	±0.006	-
$3\langle\cos\theta^r_-\rangle$	−0.110	±0.060	±0.024	±0.008	±0.050	±0.010	±0.015
$-9\langle\cos\theta^k_+\cos\theta^k_-\rangle$	0.172	±0.078	±0.041	±0.016	±0.050	±0.017	±0.027
$-9\langle\cos\theta^n_+\cos\theta^n_-\rangle$	0.427	±0.079	±0.034	±0.011	±0.065	±0.004	±0.027
$-9\langle\cos\theta^r_+\cos\theta^r_-\rangle$	0.031	±0.144	±0.055	±0.005	±0.124	±0.020	±0.033
$-9\langle\cos\theta^n_+\cos\theta^k_- + \cos\theta^k_+\cos\theta^n_-\rangle$	0.024	±0.132	±0.078	±0.004	±0.085	±0.025	-
$-9\langle\cos\theta^n_+\cos\theta^k_- - \cos\theta^k_+\cos\theta^n_-\rangle$	−0.047	±0.096	±0.059	±0.004	±0.065	±0.002	-
$-9\langle\cos\theta^n_+\cos\theta^r_- + \cos\theta^r_+\cos\theta^n_-\rangle$	0.113	±0.143	±0.076	±0.005	±0.108	±0.023	±0.015
$-9\langle\cos\theta^n_+\cos\theta^r_- - \cos\theta^r_+\cos\theta^n_-\rangle$	−0.030	±0.118	±0.076	±0.005	±0.077	±0.007	±0.052
$-9\langle\cos\theta^r_+\cos\theta^k_- + \cos\theta^k_+\cos\theta^r_-\rangle$	−0.187	±0.151	±0.069	±0.023	±0.122	±0.006	±0.039
$-9\langle\cos\theta^r_+\cos\theta^k_- - \cos\theta^k_+\cos\theta^r_-\rangle$	0.047	±0.128	±0.070	±0.003	±0.082	±0.010	±0.023

Table 5: Results corrected to parton level in the full phase-space and to stable-particle level in the fiducial phase-space. The central value with the total uncertainty is shown as well as the contribution from the various systematic uncertainty categories. The uncertainty from the "Background" category is not shown because it is always smaller than 0.001. The total uncertainty corresponds to the sum in quadrature of the uncertainty obtained from the unfolding procedure with marginalisation (including the background and detector modelling), the signal modelling and the "Others" category. The numbers shown for the "Detector" category correspond to the sum in quadrature of the individual estimates obtained as described in Section 6.3. The sum in quadrature of the values in the various columns thus does not necessarily match with the total uncertainty. The uncertainty related to the top quark mass is presented separately. It is shown as "-" when found to be compatible with zero.

Measurements	Fiducial phase-space	Full phase-space
B_+^k	-0.04 ± 0.01	-0.04 ± 0.01
B_-^k	-0.04 ± 0.01	-0.04 ± 0.01
B_+^n	-	-
B_-^n	-	-
B_+^r	-	-
B_-^r	0.02 ± 0.01	0.03 ± 0.01
$C(k,k)$	0.04 ± 0.01	0.06 ± 0.02
$C(n,n)$	-0.04 ± 0.03	-0.02 ± 0.03
$C(r,r)$	0.05 ± 0.03	0.06 ± 0.03
$C(n,k) + C(k,n)$	-	-
$C(n,k) - C(k,n)$	-	-
$C(n,r) + C(r,n)$	0.02 ± 0.01	0.02 ± 0.02
$C(n,r) - C(r,n)$	-0.08 ± 0.01	-0.07 ± 0.01
$C(r,k) + C(k,r)$	-0.06 ± 0.02	-0.10 ± 0.02
$C(r,k) - C(k,r)$	0.04 ± 0.03	0.04 ± 0.03

Table 6: Dependence of polarisation and spin correlation measurements on the MC top quark mass. The slope, computed from the reference value of 172.5 GeV, is indicated for each measurement with its statistical uncertainty in units of GeV^{-1}. Slopes which are compatible with zero within the uncertainty are indicated with "-".

Experiment	$\sqrt{s}$	Method	B_+^k	B_-^k	$C(k,k)$	B_+^n	B_-^n
ATLAS	8 TeV	Unfolding	-0.044 ± 0.038	-0.064 ± 0.040	0.296 ± 0.093	-0.018 ± 0.034	0.023 ± 0.042
CMS [16]	8 TeV	Unfolding	-0.022 ± 0.058		0.278 ± 0.084	-	-
ATLAS [11]	7 TeV	Template fit	-0.035 ± 0.040		-	-	-
ATLAS [10]	7 TeV	Template fit	-	-	0.23 ± 0.09	-	-
ATLAS [12]	7 TeV	Unfolding	-	-	0.315 ± 0.078	-	-
D0 [17]	1.96 TeV	Template fit	-0.102 ± 0.061		-	0.040 ± 0.034	

Table 7: Direct measurements of polarisations or spin correlations for different experiments and measurement techniques. If more than one measurement from an experiment is performed with the same technique, the measurement with the smallest total uncertainty is shown. If a measurement quotes polarisation values for a CP-conserving and a CP-violating production mechanism, the result for the CP-conserving case is shown in the table (P and C denote the parity and charge-conjugation transformations, respectively). The template fits for the polarisation observables usually use the information of both the top and antitop quark decay chains. In this case, only one polarisation value can be quoted as the result and is shown for both columns of polarisation along the same axis. The SM predictions of the polarisations at the Tevatron are slightly different [17, 72] due to the different dominant production mechanism, which is $q\bar{q}$ annihilation. Dashes indicate no measurement for the corresponding analysis.

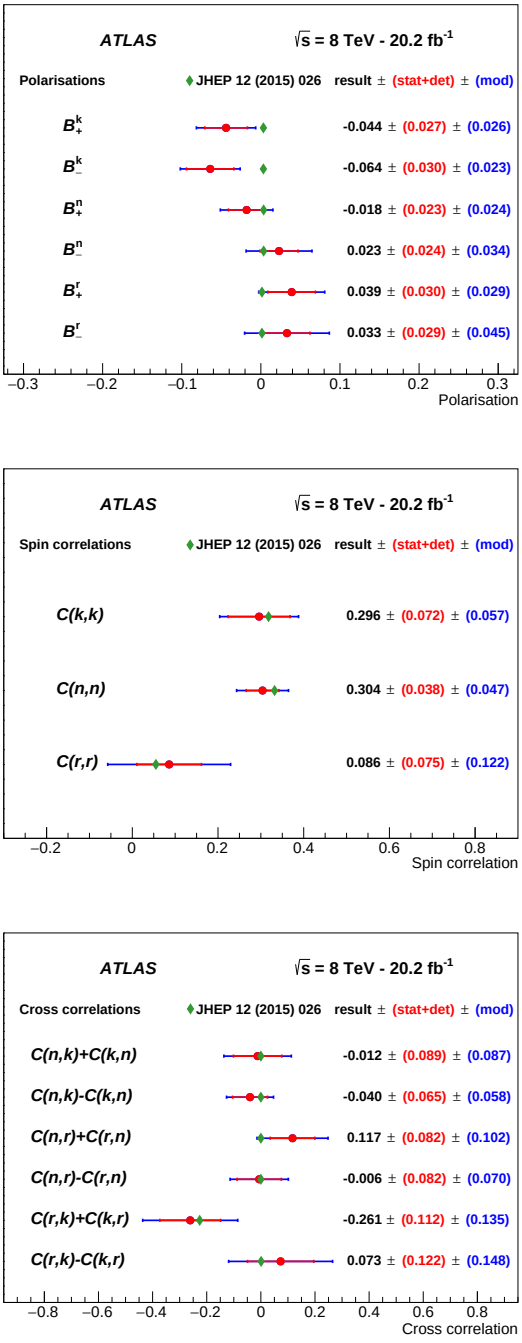

Figure 5: Comparison of the measured polarisations and spin correlations (data points) with predictions from the SM (diamonds) for the parton-level measurement. Inner bars indicate uncertainties obtained from the marginalisation, outer bars indicate modelling systematics, summed in quadrature. The widths of the diamonds are chosen for illustrative purposes only.

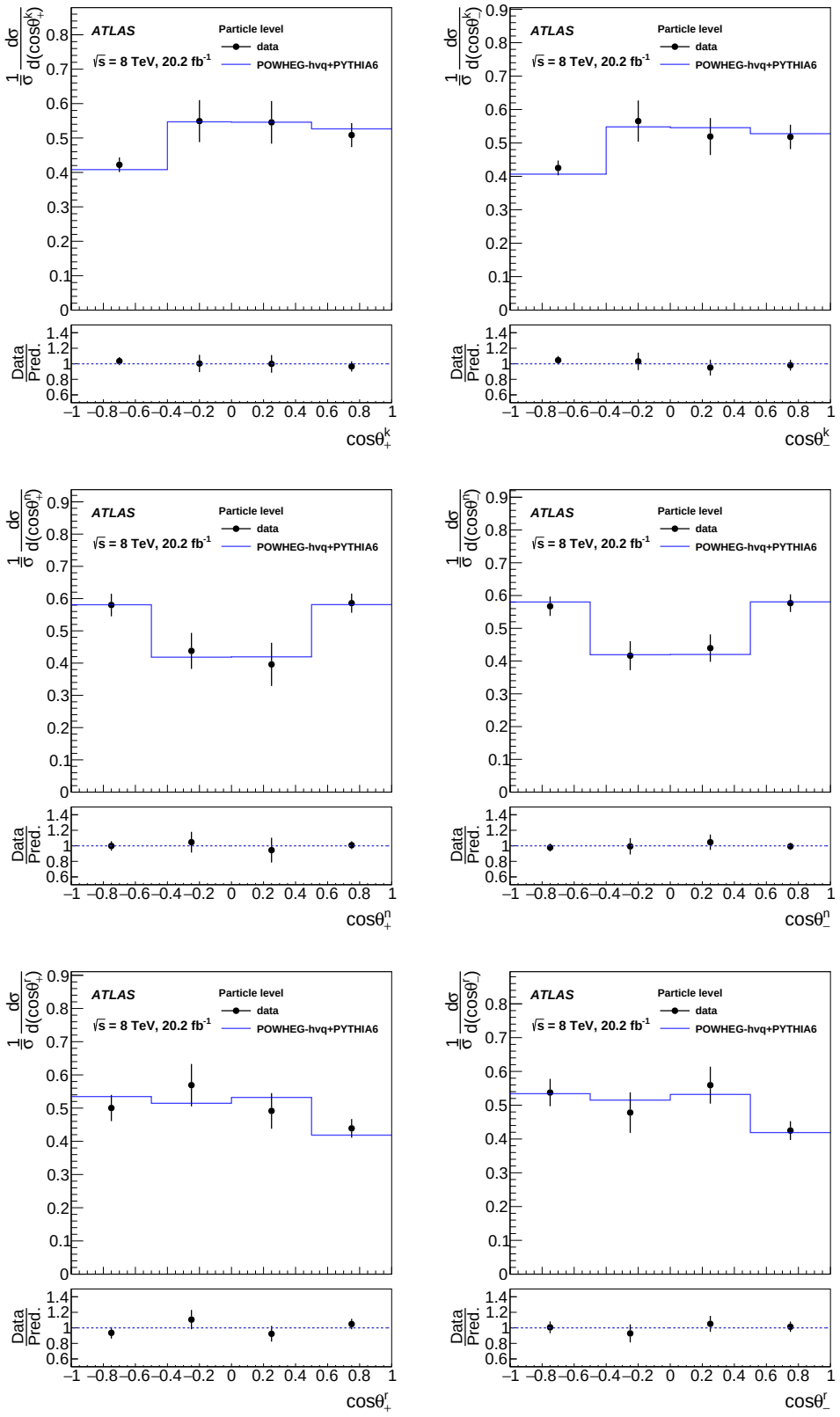

Figure 6: Comparison of the unfolded polarisation distributions and the prediction from the signal MC simulation for the stable-particle measurement. The total uncertainty is shown in each bin. The bin-to-bin correlations between adjacent bins are typically between −0.9 and −0.6. The correlations between non-adjacent bins range from −0.4 to 0.6.

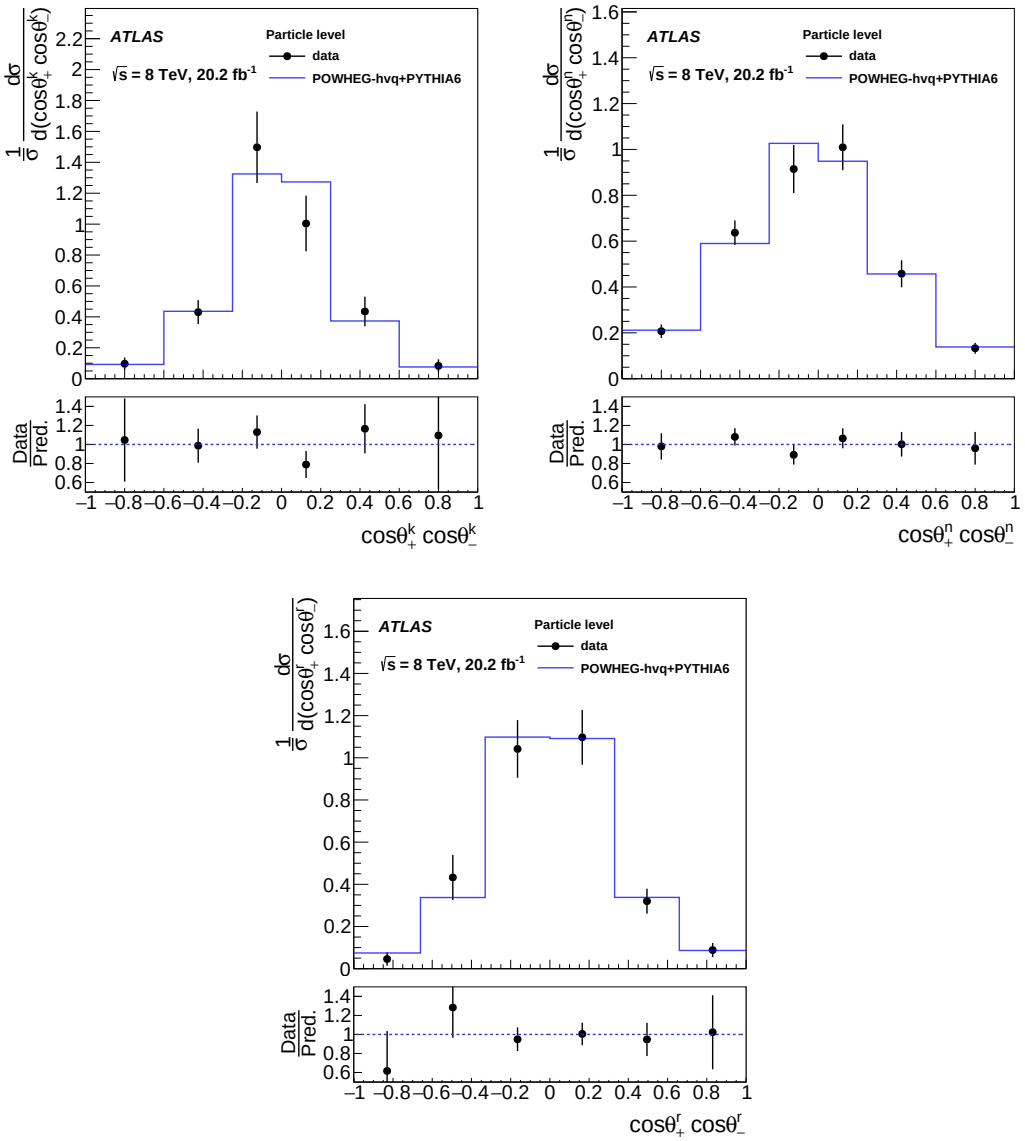

Figure 7: Comparison of the unfolded spin correlation distributions and the prediction from the signal MC simulation for the stable-particle measurement. The total uncertainty is shown in each bin. The bin-to-bin correlations between adjacent bins are typically between −0.9 and −0.4. The correlations between non-adjacent bins range from −0.4 to 0.6.

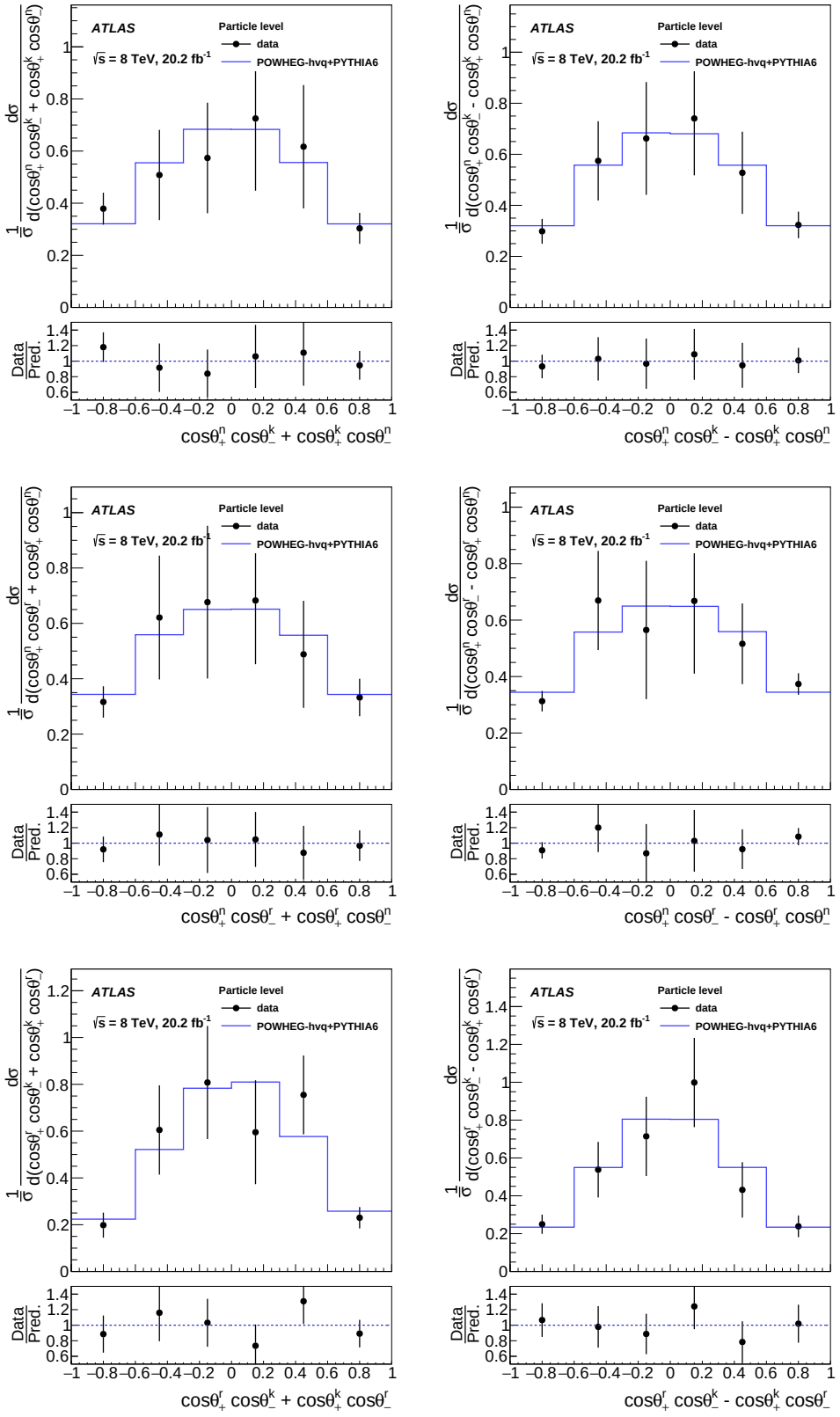

Figure 8: Comparison of the unfolded cross correlation distributions and the prediction from the signal MC simulation for the stable-particle measurement. The total uncertainty is shown in each bin. The bin-to-bin correlations between adjacent bins are typically between −0.9 and −0.7. The correlations between non-adjacent bins range from −0.4 to 0.6.

8 Conclusion

A measurement of 15 top quark spin observables was performed using a data set of 20.2 fb^{-1} of proton–proton collisions at $\sqrt{s} = 8$ TeV, recorded by the ATLAS detector at the LHC. The analysis is performed in the dilepton final state, characterised by the presence of two isolated leptons. Each of the observables is sensitive to a different coefficient of the spin density matrix of $t\bar{t}$ production. The observable distributions are corrected back to the parton and stable-particle level. At parton level, the measurements along the helicity axis are

$$\begin{aligned} B_+^k &= -0.044 \pm 0.038\ [\pm 0.027\ (\text{mass})], \\ B_-^k &= -0.064 \pm 0.040\ [\pm 0.027\ (\text{mass})], \\ C(k,k) &= 0.296 \pm 0.093\ [\pm 0.037\ (\text{mass})]. \end{aligned}$$

These values are in good agreement with the NLO SM predictions of $B_+^k = 0.0030 \pm 0.0010$, $B_-^k = 0.0034 \pm 0.0010$ and $C(k,k) = 0.318 \pm 0.003$. The spin correlation along the transverse axis differs from zero with a significance of 5.1 σ. At stable-particle level, the unfolded distributions are compared to their prediction from MC simulation (Powheg-hvq +Pythia6). All distributions are in agreement with the predictions.

Acknowledgements

We thank CERN for the very successful operation of the LHC, as well as the support staff from our institutions without whom ATLAS could not be operated efficiently.

We acknowledge the support of ANPCyT, Argentina; YerPhI, Armenia; ARC, Australia; BMWFW and FWF, Austria; ANAS, Azerbaijan; SSTC, Belarus; CNPq and FAPESP, Brazil; NSERC, NRC and CFI, Canada; CERN; CONICYT, Chile; CAS, MOST and NSFC, China; COLCIENCIAS, Colombia; MSMT CR, MPO CR and VSC CR, Czech Republic; DNRF and DNSRC, Denmark; IN2P3-CNRS, CEA-DSM/IRFU, France; GNSF, Georgia; BMBF, HGF, and MPG, Germany; GSRT, Greece; RGC, Hong Kong SAR, China; ISF, I-CORE and Benoziyo Center, Israel; INFN, Italy; MEXT and JSPS, Japan; CNRST, Morocco; FOM and NWO, Netherlands; RCN, Norway; MNiSW and NCN, Poland; FCT, Portugal; MNE/IFA, Romania; MES of Russia and NRC KI, Russian Federation; JINR; MESTD, Serbia; MSSR, Slovakia; ARRS and MIZŠ, Slovenia; DST/NRF, South Africa; MINECO, Spain; SRC and Wallenberg Foundation, Sweden; SERI, SNSF and Cantons of Bern and Geneva, Switzerland; MOST, Taiwan; TAEK, Turkey; STFC, United Kingdom; DOE and NSF, United States of America. In addition, individual groups and members have received support from BCKDF, the Canada Council, CANARIE, CRC, Compute Canada, FQRNT, and the Ontario Innovation Trust, Canada; EPLANET, ERC, ERDF, FP7, Horizon 2020 and Marie Skłodowska-Curie Actions, European Union; Investissements d'Avenir Labex and Idex, ANR, Région Auvergne and Fondation Partager le Savoir, France; DFG and AvH Foundation, Germany; Herakleitos, Thales and Aristeia programmes co-financed by EU-ESF and the Greek NSRF; BSF, GIF and Minerva, Israel; BRF, Norway; CERCA Programme Generalitat de Catalunya, Generalitat Valenciana, Spain; the Royal Society and Leverhulme Trust, United Kingdom.

The crucial computing support from all WLCG partners is acknowledged gratefully, in particular from CERN, the ATLAS Tier-1 facilities at TRIUMF (Canada), NDGF (Denmark, Norway, Sweden), CC-IN2P3 (France), KIT/GridKA (Germany), INFN-CNAF (Italy), NL-T1 (Netherlands), PIC (Spain), ASGC

(Taiwan), RAL (UK) and BNL (USA), the Tier-2 facilities worldwide and large non-WLCG resource providers. Major contributors of computing resources are listed in Ref. [73].

References

[1] CDF Collaboration, T. Aaltonen et al.,
Observation of Top Quark Production in $\bar{p}p$ Collisions with the Collider Detector at Fermilab,
Phys. Rev. Lett. **74** (1995) 2626–2631, arXiv: hep-ex/9503002 [hep-ex].

[2] D0 Collaboration, S. Abachi et al.,
Search for High Mass Top Quark Production in $p\bar{p}$ Collisions at $\sqrt{s} = 1.8$ TeV,
Phys. Rev. Lett. **74** (1995) 2422–2426, arXiv: hep-ex/9411001 [hep-ex].

[3] M. Jezabek and J. H. Kuhn, *The Top width: Theoretical update*,
Phys. Rev. D **48** (1993) 1910–1913, [Erratum: Phys. Rev. D 49, 4970 (1994)],
arXiv: hep-ph/9302295 [hep-ph].

[4] D0 Collaboration, V. M. Abazov et al., *An Improved determination of the width of the top quark*,
Phys. Rev. D **85** (2012) 091104, arXiv: 1201.4156 [hep-ex].

[5] CDF Collaboration, T. Aaltonen et al., *Direct Top-Quark Width Measurement CDF*,
Phys. Rev. Lett. **105** (2010) 232003, arXiv: 1008.3891 [hep-ex].

[6] W. Bernreuther and Z.-G. Si, *Top quark spin correlations and polarization at the LHC: standard model predictions and effects of anomalous top chromo moments*,
Phys. Lett. B **725** (2013) 115–122, [Erratum: Phys. Lett. B 744, 413 (2015)],
arXiv: 1305.2066 [hep-ph].

[7] S. Fajfer, J. F. Kamenik and B. Melic, *Discerning New Physics in Top-Antitop Production using Top Spin Observables at Hadron Colliders*, JHEP **08** (2012) 114, arXiv: 1205.0264 [hep-ph].

[8] R. M. Godbole, L. Hartgring, I. Niessen and C. D. White,
'Polarisation studies in $H^- t$ production', *Proceedings, 4th International Workshop on Prospects for Charged Higgs Discovery at Colliders (CHARGED 2012)*, 2013,
arXiv: 1301.6877 [hep-ph].

[9] G. Belanger, R. M. Godbole, S. Kraml and S. Kulkarni,
Top Polarization in Sbottom Decays at the LHC, (2013), arXiv: 1304.2987 [hep-ph].

[10] ATLAS Collaboration, *Measurements of spin correlation in top-antitop quark events from proton-proton collisions at $\sqrt{s} = 7$ TeV using the ATLAS detector*,
Phys. Rev. D **90** (2014) 112016, arXiv: 1407.4314 [hep-ex].

[11] ATLAS Collaboration, *Measurement of Top Quark Polarization in Top-Antitop Events from Proton-Proton Collisions at $\sqrt{s} = 7$ TeV Using the ATLAS Detector*,
Phys. Rev. Lett. **111** (2013) 232002, arXiv: 1307.6511 [hep-ex].

[12] ATLAS Collaboration, *Measurement of the correlations between the polar angles of leptons from top quark decays in the helicity basis at $\sqrt{s} = 7$ TeV using the ATLAS detector*,
Phys. Rev. D **93** (2016) 012002, arXiv: 1510.07478 [hep-ex].

[13] ATLAS Collaboration, *Measurement of Spin Correlation in Top-Antitop Quark Events and Search for Top Squark Pair Production in pp Collisions at $\sqrt{s} = 8$ TeV Using the ATLAS Detector*,
Phys. Rev. Lett. **114** (2015) 142001, arXiv: 1412.4742 [hep-ex].

[14] CMS Collaboration, *Measurements of $t\bar{t}$ spin correlations and top-quark polarization using dilepton final states in pp collisions at $\sqrt{s} = 7$ TeV*, Phys. Rev. Lett. **112** (2014) 182001,
arXiv: 1311.3924 [hep-ex].

[15] CMS Collaboration, *Measurement of spin correlations in $t\bar{t}$ production using the matrix element method in the muon+jets final state in pp collisions at $\sqrt{s} = 8$ TeV*, Phys. Lett. B **758** (2016) 321–346, arXiv: 1511.06170 [hep-ex].

[16] CMS Collaboration, *Measurements of $t\bar{t}$ spin correlations and top quark polarization using dilepton final states in pp collisions at $\sqrt{s} = 8$ TeV*, Phys. Rev. D **93** (2016) 052007, arXiv: 1601.01107 [hep-ex].

[17] D0 Collaboration, V. M. Abazov et al., *Measurement of top quark polarization in $t\bar{t}$ lepton+jets final states*, Phys. Rev. **D95** (2017) 011101, arXiv: 1607.07627 [hep-ex].

[18] CDF Collaboration, T. Aaltonen et al., *Measurement of $t\bar{t}$ Spin Correlation in $p\bar{p}$ Collisions Using the CDF II Detector at the Tevatron*, Phys. Rev. D **83** (2011) 031104, arXiv: 1012.3093 [hep-ex].

[19] W. Bernreuther, D. Heisler and Z.-G. Si, *A set of top quark spin correlation and polarization observables for the LHC: Standard Model predictions and new physics contributions*, JHEP **12** (2015) 026, arXiv: 1508.05271 [hep-ph].

[20] ATLAS Collaboration, *The ATLAS Experiment at the CERN Large Hadron Collider*, JINST **3** (2008) S08003.

[21] W. Bernreuther, A. Brandenburg, Z. G. Si and P. Uwer, *Top quark pair production and decay at hadron colliders*, Nucl. Phys. B **690** (2004) 81–137, arXiv: hep-ph/0403035 [hep-ph].

[22] M. Baumgart and B. Tweedie, *Transverse Top Quark Polarization and the $t\bar{t}$ Forward-Backward Asymmetry*, JHEP **08** (2013) 072, arXiv: 1303.1200 [hep-ph].

[23] *First combination of Tevatron and LHC measurements of the top-quark mass*, (2014), arXiv: 1403.4427 [hep-ex].

[24] S. Frixione, P. Nason and C. Oleari, *Matching NLO QCD computations with Parton Shower simulations: the POWHEG method*, JHEP **11** (2007) 070, arXiv: 0709.2092 [hep-ph].

[25] P. Nason, *A New method for combining NLO QCD with shower Monte Carlo algorithms*, JHEP **11** (2004) 040, arXiv: hep-ph/0409146 [hep-ph].

[26] S. Alioli, P. Nason, C. Oleari and E. Re, *A general framework for implementing NLO calculations in shower Monte Carlo programs: the POWHEG BOX*, JHEP **06** (2010) 043, arXiv: 1002.2581 [hep-ph].

[27] S. Frixione, P. Nason and G. Ridolfi, *A Positive-weight next-to-leading-order Monte Carlo for heavy flavour hadroproduction*, JHEP **09** (2007) 126, arXiv: 0707.3088 [hep-ph].

[28] ATLAS Collaboration, *Comparison of Monte Carlo generator predictions to ATLAS measurements of top pair production at 7 TeV*, ATL-PHYS-PUB-2015-002 (2015), URL: https://cds.cern.ch/record/1981319.

[29] ATLAS Collaboration, *Comparison of Monte Carlo generator predictions from Powheg and Sherpa to ATLAS measurements of top pair production at 7 TeV*, ATL-PHYS-PUB-2015-011 (2015), URL: https://cds.cern.ch/record/2020602.

[30] H.-L. Lai et al., *New parton distributions for collider physics*, Phys. Rev. D **82** (2010) 074024, arXiv: 1007.2241 [hep-ph].

[31] T. Sjöstrand, S. Mrenna and P. Z. Skands, *PYTHIA 6.4 Physics and Manual*, JHEP **05** (2006) 026, arXiv: hep-ph/0603175 [hep-ph].

[32] P. Z. Skands, *Tuning Monte Carlo Generators: The Perugia Tunes*, Phys. Rev. D **82** (2010) 074018, arXiv: 1005.3457 [hep-ph].

[33] ATLAS Collaboration, *The ATLAS Simulation Infrastructure*, Eur. Phys. J. C **70** (2010) 823–874, arXiv: 1005.4568 [physics.ins-det].

[34] S. Agostinelli et al., *GEANT4: A Simulation toolkit*, Nucl. Instrum. Meth. A **506** (2003) 250–303.

[35] ATLAS Collaboration, *The simulation principle and performance of the ATLAS fast calorimeter simulation FastCaloSim*, ATL-PHYS-PUB-2010-013 (2010), URL: https://cds.cern.ch/record/1300517.

[36] E. Re, *Single-top Wt-channel production matched with parton showers using the POWHEG method*, Eur. Phys. J. C **71** (2011) 1547, arXiv: 1009.2450 [hep-ph].

[37] J. Pumplin et al., *New generation of parton distributions with uncertainties from global QCD analysis*, JHEP **07** (2002) 012.

[38] ATLAS Collaboration, *New ATLAS event generator tunes to 2010 data*, ATL-PHYS-PUB-2011-008 (2011), URL: https://cds.cern.ch/record/1345343.

[39] M. L. Mangano, M. Moretti, F. Piccinini, R. Pittau and A. D. Polosa, *ALPGEN, a generator for hard multiparton processes in hadronic collisions*, JHEP **07** (2003) 001, arXiv: hep-ph/0206293 [hep-ph].

[40] J. Alwall, M. Herquet, F. Maltoni, O. Mattelaer and T. Stelzer, *MadGraph 5 : Going Beyond*, JHEP **06** (2011) 128, arXiv: 1106.0522 [hep-ph].

[41] J. M. Butterworth et al., *Multiparton interactions in photoproduction at HERA*, Z. Phys. C **72** (1996) 637–646.

[42] T. Sjöstrand, S. Mrenna and P. Z. Skands, *A Brief Introduction to PYTHIA 8.1*, Comput. Phys. Commun. **178** (2008) 852–867, arXiv: 0710.3820 [hep-ph].

[43] S. Frixione and B. R. Webber, *Matching NLO QCD computations and parton shower simulations*, JHEP **06** (2002) 029, arXiv: hep-ph/0204244 [hep-ph].

[44] S. Frixione, P. Nason and B. R. Webber, *Matching NLO QCD and parton showers in heavy flavor production*, JHEP **08** (2003) 007, arXiv: hep-ph/0305252 [hep-ph].

[45] ATLAS Collaboration, *Electron efficiency measurements with the ATLAS detector using 2012 LHC proton-proton collision data*, (2016), arXiv: 1612.01456 [hep-ex].

[46] ATLAS Collaboration, *Measurement of the muon reconstruction performance of the ATLAS detector using 2011 and 2012 LHC proton–proton collision data*, Eur. Phys. J. C **74** (2014) 3130, arXiv: 1407.3935 [hep-ex].

[47] M. Cacciari, G. P. Salam and G. Soyez, *The anti-k_t jet clustering algorithm*, JHEP **04** (2008) 063, arXiv: 0802.1189 [hep-ph].

[48] ATLAS Collaboration, *Jet energy measurement and its systematic uncertainty in proton –proton collisions at $\sqrt{s}$ = 7 TeV with the ATLAS detector*, Eur. Phys. J. C **75** (2015) 17, arXiv: 1406.0076 [hep-ex].

[49] ATLAS Collaboration, *Performance of b-Jet Identification in the ATLAS Experiment*, JINST **11** (2016) P04008, arXiv: 1512.01094 [hep-ex].

[50] ATLAS Collaboration, *Performance of Missing Transverse Momentum Reconstruction in Proton-Proton Collisions at 7 TeV with ATLAS*, Eur. Phys. J. C **72** (2012) 1844, arXiv: 1108.5602 [hep-ex].

[51] D0 Collaboration, B. Abbott et al., *Measurement of the top quark mass using dilepton events*, Phys. Rev. Lett. **80** (1998) 2063–2068, arXiv: hep-ex/9706014 [hep-ex].

[52] ATLAS Collaboration, *Measurement of the charge asymmetry in dileptonic decays of top quark pairs in pp collisions at $\sqrt{s}$ = 7 TeV using the ATLAS detector*, JHEP **05** (2015) 061, arXiv: 1501.07383 [hep-ex].

[53] C. Patrignani et al., *Review of Particle Physics*, Chin. Phys. C **40** (2016) 100001.

[54] M. Cacciari, G. P. Salam and G. Soyez, *The Catchment Area of Jets*, JHEP **04** (2008) 005, arXiv: 0802.1188 [hep-ph].

[55] ATLAS Collaboration, *Differential top-antitop cross-section measurements as a function of observables constructed from final-state particles using pp collisions at $\sqrt{s}$ = 7 TeV in the ATLAS detector*, JHEP **06** (2015) 100, arXiv: 1502.05923 [hep-ex].

[56] G. Choudalakis, *Fully Bayesian Unfolding*, (2012), arXiv: 1201.4612 [physics.data-an].

[57] ATLAS Collaboration, *Performance of the ATLAS Trigger System in 2010*, Eur. Phys. J. C **72** (2012) 1849, arXiv: 1110.1530 [hep-ex].

[58] ATLAS Collaboration, *Electron reconstruction and identification efficiency measurements with the ATLAS detector using the 2011 LHC proton-proton collision data*, Eur. Phys. J. C **74** (2014) 2941, arXiv: 1404.2240 [hep-ex].

[59] ATLAS Collaboration, *Calibration of the performance of b-tagging for c and light-flavour jets in the 2012 ATLAS data*, ATLAS-CONF-2014-046 (2014), URL: https://cds.cern.ch/record/1741020.

[60] ATLAS Collaboration, *Calibration of b-tagging using dileptonic top pair events in a combinatorial likelihood approach with the ATLAS experiment*, ATLAS-CONF-2014-004 (2014), URL: https://cds.cern.ch/record/1664335.

[61] ATLAS Collaboration, *Performance of Missing Transverse Momentum Reconstruction in ATLAS studied in Proton-Proton Collisions recorded in 2012 at 8 TeV*, (2013), URL: https://cds.cern.ch/record/1570993.

[62] N. Kidonakis, 'Differential and total cross sections for top pair and single top production', *Proceedings, 20th International Workshop on Deep-Inelastic Scattering and Related Subjects (DIS 2012)*, 2012 831–834, arXiv: 1205.3453 [hep-ph].

[63] J. M. Campbell and R. K. Ellis, *$t\bar{t}W^{\pm}$ production and decay at NLO*, JHEP **07** (2012) 052, arXiv: 1204.5678 [hep-ph].

[64] M. V. Garzelli, A. Kardos, C. G. Papadopoulos and Z. Trocsanyi, *$t\bar{t}W^{\pm}$ and $t\bar{t}Z$ Hadroproduction at NLO accuracy in QCD with Parton Shower and Hadronization effects*, JHEP **11** (2012) 056, arXiv: 1208.2665 [hep-ph].

[65] ATLAS Collaboration, *Measurement of $t\bar{t}$ production with a veto on additional central jet activity in pp collisions at $\sqrt{s} = 7$ TeV using the ATLAS detector*, Eur. Phys. J. C **72** (2012) 2043.

[66] A. D. Martin, W. J. Stirling, R. S. Thorne and G. Watt, *Parton distributions for the LHC*, Eur. Phys. J. C **63** (2009) 189–285, arXiv: 0901.0002 [hep-ph].

[67] R. D. Ball et al., *Parton distributions with LHC data*, Nucl. Phys. B **867** (2013) 244–289, arXiv: 1207.1303 [hep-ph].

[68] M. Botje et al., *The PDF4LHC Working Group Interim Recommendations*, (2011), arXiv: 1101.0538 [hep-ph].

[69] ATLAS Collaboration, *Measurements of top-quark pair differential cross-sections in the lepton+jets channel in pp collisions at $\sqrt{s} = 8$ TeV using the ATLAS detector*, Eur. Phys. J. C **76** (2016) 538, arXiv: 1511.04716 [hep-ex].

[70] CMS Collaboration, *Measurement of the differential cross section for top quark pair production in pp collisions at $\sqrt{s} = 8$ TeV*, Eur. Phys. J. C **75** (2015) 542, arXiv: 1505.04480 [hep-ex].

[71] ATLAS Collaboration, *Measurement of the top quark mass in the $t\bar{t} \to$ dilepton channel from $\sqrt{s} = 8$ TeV ATLAS data*, Phys. Lett. B **761** (2016) 350–371, arXiv: 1606.02179 [hep-ex].

[72] M. Baumgart and B. Tweedie, *Transverse Top Quark Polarization and the $t\bar{t}$ Forward-Backward Asymmetry*, JHEP **08** (2013) 072, arXiv: 1303.1200 [hep-ph].

[73] ATLAS Collaboration, *ATLAS Computing Acknowledgements 2016–2017*, ATL-GEN-PUB-2016-002, URL: https://cds.cern.ch/record/2202407.

The ATLAS Collaboration

M. Aaboud[137d], G. Aad[88], B. Abbott[115], J. Abdallah[8], O. Abdinov[12], B. Abeloos[119], O.S. AbouZeid[139], N.L. Abraham[151], H. Abramowicz[155], H. Abreu[154], R. Abreu[118], Y. Abulaiti[148a,148b], B.S. Acharya[167a,167b,a], S. Adachi[157], L. Adamczyk[41a], D.L. Adams[27], J. Adelman[110], S. Adomeit[102], T. Adye[133], A.A. Affolder[139], T. Agatonovic-Jovin[14], J.A. Aguilar-Saavedra[128a,128f], S.P. Ahlen[24], F. Ahmadov[68,b], G. Aielli[135a,135b], H. Akerstedt[148a,148b], T.P.A. Åkesson[84], A.V. Akimov[98], G.L. Alberghi[22a,22b], J. Albert[172], S. Albrand[58], M.J. Alconada Verzini[74], M. Aleksa[32], I.N. Aleksandrov[68], C. Alexa[28b], G. Alexander[155], T. Alexopoulos[10], M. Alhroob[115], B. Ali[130], M. Aliev[76a,76b], G. Alimonti[94a], J. Alison[33], S.P. Alkire[38], B.M.M. Allbrooke[151], B.W. Allen[118], P.P. Allport[19], A. Aloisio[106a,106b], A. Alonso[39], F. Alonso[74], C. Alpigiani[140], A.A. Alshehri[56], M. Alstaty[88], B. Alvarez Gonzalez[32], D. Álvarez Piqueras[170], M.G. Alviggi[106a,106b], B.T. Amadio[16], Y. Amaral Coutinho[26a], C. Amelung[25], D. Amidei[92], S.P. Amor Dos Santos[128a,128c], A. Amorim[128a,128b], S. Amoroso[32], G. Amundsen[25], C. Anastopoulos[141], L.S. Ancu[52], N. Andari[19], T. Andeen[11], C.F. Anders[60b], J.K. Anders[77], K.J. Anderson[33], A. Andreazza[94a,94b], V. Andrei[60a], S. Angelidakis[9], I. Angelozzi[109], A. Angerami[38], F. Anghinolfi[32], A.V. Anisenkov[111,c], N. Anjos[13], A. Annovi[126a,126b], C. Antel[60a], M. Antonelli[50], A. Antonov[100,*], D.J. Antrim[166], F. Anulli[134a], M. Aoki[69], L. Aperio Bella[19], G. Arabidze[93], Y. Arai[69], J.P. Araque[128a], V. Araujo Ferraz[26a], A.T.H. Arce[48], F.A. Arduh[74], J-F. Arguin[97], S. Argyropoulos[66], M. Arik[20a], A.J. Armbruster[145], L.J. Armitage[79], O. Arnaez[32], H. Arnold[51], M. Arratia[30], O. Arslan[23], A. Artamonov[99], G. Artoni[122], S. Artz[86], S. Asai[157], N. Asbah[45], A. Ashkenazi[155], B. Åsman[148a,148b], L. Asquith[151], K. Assamagan[27], R. Astalos[146a], M. Atkinson[169], N.B. Atlay[143], K. Augsten[130], G. Avolio[32], B. Axen[16], M.K. Ayoub[119], G. Azuelos[97,d], M.A. Baak[32], A.E. Baas[60a], M.J. Baca[19], H. Bachacou[138], K. Bachas[76a,76b], M. Backes[122], M. Backhaus[32], P. Bagiacchi[134a,134b], P. Bagnaia[134a,134b], Y. Bai[35a], J.T. Baines[133], M. Bajic[39], O.K. Baker[179], E.M. Baldin[111,c], P. Balek[175], T. Balestri[150], F. Balli[138], W.K. Balunas[124], E. Banas[42], Sw. Banerjee[176,e], A.A.E. Bannoura[178], L. Barak[32], E.L. Barberio[91], D. Barberis[53a,53b], M. Barbero[88], T. Barillari[103], M-S Barisits[32], T. Barklow[145], N. Barlow[30], S.L. Barnes[87], B.M. Barnett[133], R.M. Barnett[16], Z. Barnovska-Blenessy[36a], A. Baroncelli[136a], G. Barone[25], A.J. Barr[122], L. Barranco Navarro[170], F. Barreiro[85], J. Barreiro Guimarães da Costa[35a], R. Bartoldus[145], A.E. Barton[75], P. Bartos[146a], A. Basalaev[125], A. Bassalat[119,f], R.L. Bates[56], S.J. Batista[161], J.R. Batley[30], M. Battaglia[139], M. Bauce[134a,134b], F. Bauer[138], H.S. Bawa[145,g], J.B. Beacham[113], M.D. Beattie[75], T. Beau[83], P.H. Beauchemin[165], P. Bechtle[23], H.P. Beck[18,h], K. Becker[122], M. Becker[86], M. Beckingham[173], C. Becot[112], A.J. Beddall[20e], A. Beddall[20b], V.A. Bednyakov[68], M. Bedognetti[109], C.P. Bee[150], L.J. Beemster[109], T.A. Beermann[32], M. Begel[27], J.K. Behr[45], A.S. Bell[81], G. Bella[155], L. Bellagamba[22a], A. Bellerive[31], M. Bellomo[89], K. Belotskiy[100], O. Beltramello[32], N.L. Belyaev[100], O. Benary[155,*], D. Benchekroun[137a], M. Bender[102], K. Bendtz[148a,148b], N. Benekos[10], Y. Benhammou[155], E. Benhar Noccioli[179], J. Benitez[66], D.P. Benjamin[48], J.R. Bensinger[25], S. Bentvelsen[109], L. Beresford[122], M. Beretta[50], D. Berge[109], E. Bergeaas Kuutmann[168], N. Berger[5], J. Beringer[16], S. Berlendis[58], N.R. Bernard[89], C. Bernius[112], F.U. Bernlochner[23], W. Bernreuther[i], T. Berry[80], P. Berta[131], C. Bertella[86], G. Bertoli[148a,148b], F. Bertolucci[126a,126b], I.A. Bertram[75], C. Bertsche[45], D. Bertsche[115], G.J. Besjes[39], O. Bessidskaia Bylund[148a,148b], M. Bessner[45], N. Besson[138], C. Betancourt[51], A. Bethani[58], S. Bethke[103], A.J. Bevan[79], R.M. Bianchi[127], M. Bianco[32], O. Biebel[102], D. Biedermann[17], R. Bielski[87], N.V. Biesuz[126a,126b], M. Biglietti[136a], J. Bilbao De Mendizabal[52], T.R.V. Billoud[97], H. Bilokon[50], M. Bindi[57], A. Bingul[20b], C. Bini[134a,134b], S. Biondi[22a,22b], T. Bisanz[57], D.M. Bjergaard[48], C.W. Black[152], J.E. Black[145], K.M. Black[24], D. Blackburn[140], R.E. Blair[6], T. Blazek[146a], I. Bloch[45], C. Blocker[25], A. Blue[56], W. Blum[86,*], U. Blumenschein[57], S. Blunier[34a],

G.J. Bobbink[109], V.S. Bobrovnikov[111,c], S.S. Bocchetta[84], A. Bocci[48], C. Bock[102], M. Boehler[51], D. Boerner[178], J.A. Bogaerts[32], D. Bogavac[102], A.G. Bogdanchikov[111], C. Bohm[148a], V. Boisvert[80], P. Bokan[14], T. Bold[41a], A.S. Boldyrev[101], M. Bomben[83], M. Bona[79], M. Boonekamp[138], A. Borisov[132], G. Borissov[75], J. Bortfeldt[32], D. Bortoletto[122], V. Bortolotto[62a,62b,62c], K. Bos[109], D. Boscherini[22a], M. Bosman[13], J.D. Bossio Sola[29], J. Boudreau[127], J. Bouffard[2], E.V. Bouhova-Thacker[75], D. Boumediene[37], C. Bourdarios[119], S.K. Boutle[56], A. Boveia[113], J. Boyd[32], I.R. Boyko[68], J. Bracinik[19], A. Brandt[8], G. Brandt[57], O. Brandt[60a], U. Bratzler[158], B. Brau[89], J.E. Brau[118], W.D. Breaden Madden[56], K. Brendlinger[124], A.J. Brennan[91], L. Brenner[109], R. Brenner[168], S. Bressler[175], T.M. Bristow[49], D. Britton[56], D. Britzger[45], F.M. Brochu[30], I. Brock[23], R. Brock[93], G. Brooijmans[38], T. Brooks[80], W.K. Brooks[34b], J. Brosamer[16], E. Brost[110], J.H Broughton[19], P.A. Bruckman de Renstrom[42], D. Bruncko[146b], R. Bruneliere[51], A. Bruni[22a], G. Bruni[22a], L.S. Bruni[109], BH Brunt[30], M. Bruschi[22a], N. Bruscino[23], P. Bryant[33], L. Bryngemark[84], T. Buanes[15], Q. Buat[144], P. Buchholz[143], A.G. Buckley[56], I.A. Budagov[68], F. Buehrer[51], M.K. Bugge[121], O. Bulekov[100], D. Bullock[8], H. Burckhart[32], S. Burdin[77], C.D. Burgard[51], A.M. Burger[5], B. Burghgrave[110], K. Burka[42], S. Burke[133], I. Burmeister[46], J.T.P. Burr[122], E. Busato[37], D. Büscher[51], V. Büscher[86], P. Bussey[56], J.M. Butler[24], C.M. Buttar[56], J.M. Butterworth[81], P. Butti[32], W. Buttinger[27], A. Buzatu[56], A.R. Buzykaev[111,c], S. Cabrera Urbán[170], D. Caforio[130], V.M. Cairo[40a,40b], O. Cakir[4a], N. Calace[52], P. Calafiura[16], A. Calandri[88], G. Calderini[83], P. Calfayan[64], G. Callea[40a,40b], L.P. Caloba[26a], S. Calvente Lopez[85], D. Calvet[37], S. Calvet[37], T.P. Calvet[88], R. Camacho Toro[33], S. Camarda[32], P. Camarri[135a,135b], D. Cameron[121], R. Caminal Armadans[169], C. Camincher[58], S. Campana[32], M. Campanelli[81], A. Camplani[94a,94b], A. Campoverde[143], V. Canale[106a,106b], A. Canepa[163a], M. Cano Bret[36c], J. Cantero[116], T. Cao[155], M.D.M. Capeans Garrido[32], I. Caprini[28b], M. Caprini[28b], M. Capua[40a,40b], R.M. Carbone[38], R. Cardarelli[135a], F. Cardillo[51], I. Carli[131], T. Carli[32], G. Carlino[106a], B.T. Carlson[127], L. Carminati[94a,94b], R.M.D. Carney[148a,148b], S. Caron[108], E. Carquin[34b], G.D. Carrillo-Montoya[32], J.R. Carter[30], J. Carvalho[128a,128c], D. Casadei[19], M.P. Casado[13,j], M. Casolino[13], D.W. Casper[166], E. Castaneda-Miranda[147a], R. Castelijn[109], A. Castelli[109], V. Castillo Gimenez[170], N.F. Castro[128a,k], A. Catinaccio[32], J.R. Catmore[121], A. Cattai[32], J. Caudron[23], V. Cavaliere[169], E. Cavallaro[13], D. Cavalli[94a], M. Cavalli-Sforza[13], V. Cavasinni[126a,126b], F. Ceradini[136a,136b], L. Cerda Alberich[170], A.S. Cerqueira[26b], A. Cerri[151], L. Cerrito[135a,135b], F. Cerutti[16], A. Cervelli[18], S.A. Cetin[20d], A. Chafaq[137a], D. Chakraborty[110], S.K. Chan[59], Y.L. Chan[62a], P. Chang[169], J.D. Chapman[30], D.G. Charlton[19], A. Chatterjee[52], C.C. Chau[161], C.A. Chavez Barajas[151], S. Che[113], S. Cheatham[167a,167c], A. Chegwidden[93], S. Chekanov[6], S.V. Chekulaev[163a], G.A. Chelkov[68,l], M.A. Chelstowska[92], C. Chen[67], H. Chen[27], S. Chen[35b], S. Chen[157], X. Chen[35c,m], Y. Chen[70], H.C. Cheng[92], H.J. Cheng[35a], Y. Cheng[33], A. Cheplakov[68], E. Cheremushkina[132], R. Cherkaoui El Moursli[137e], V. Chernyatin[27,*], E. Cheu[7], L. Chevalier[138], V. Chiarella[50], G. Chiarelli[126a,126b], G. Chiodini[76a], A.S. Chisholm[32], A. Chitan[28b], Y.H. Chiu[172], M.V. Chizhov[68], K. Choi[64], A.R. Chomont[37], S. Chouridou[9], B.K.B. Chow[102], V. Christodoulou[81], D. Chromek-Burckhart[32], J. Chudoba[129], A.J. Chuinard[90], J.J. Chwastowski[42], L. Chytka[117], A.K. Ciftci[4a], D. Cinca[46], V. Cindro[78], I.A. Cioara[23], C. Ciocca[22a,22b], A. Ciocio[16], F. Cirotto[106a,106b], Z.H. Citron[175], M. Citterio[94a], M. Ciubancan[28b], A. Clark[52], B.L. Clark[59], M.R. Clark[38], P.J. Clark[49], R.N. Clarke[16], C. Clement[148a,148b], Y. Coadou[88], M. Cobal[167a,167c], A. Coccaro[52], J. Cochran[67], L. Colasurdo[108], B. Cole[38], A.P. Colijn[109], J. Collot[58], T. Colombo[166], P. Conde Muiño[128a,128b], E. Coniavitis[51], S.H. Connell[147b], I.A. Connelly[80], V. Consorti[51], S. Constantinescu[28b], G. Conti[32], F. Conventi[106a,n], M. Cooke[16], B.D. Cooper[81], A.M. Cooper-Sarkar[122], F. Cormier[171], K.J.R. Cormier[161], T. Cornelissen[178], M. Corradi[134a,134b], F. Corriveau[90,o], A. Cortes-Gonzalez[32], G. Cortiana[103], G. Costa[94a], M.J. Costa[170], D. Costanzo[141], G. Cottin[30], G. Cowan[80], B.E. Cox[87], K. Cranmer[112], S.J. Crawley[56], G. Cree[31], S. Crépé-Renaudin[58], F. Crescioli[83], W.A. Cribbs[148a,148b],

M. Crispin Ortuzar[122], M. Cristinziani[23], V. Croft[108], G. Crosetti[40a,40b], A. Cueto[85], T. Cuhadar Donszelmann[141], J. Cummings[179], M. Curatolo[50], J. Cúth[86], H. Czirr[143], P. Czodrowski[3], G. D'amen[22a,22b], S. D'Auria[56], M. D'Onofrio[77], M.J. Da Cunha Sargedas De Sousa[128a,128b], C. Da Via[87], W. Dabrowski[41a], T. Dado[146a], T. Dai[92], O. Dale[15], F. Dallaire[97], C. Dallapiccola[89], M. Dam[39], J.R. Dandoy[33], N.P. Dang[51], A.C. Daniells[19], N.S. Dann[87], M. Danninger[171], M. Dano Hoffmann[138], V. Dao[51], G. Darbo[53a], S. Darmora[8], J. Dassoulas[3], A. Dattagupta[118], W. Davey[23], C. David[45], T. Davidek[131], M. Davies[155], P. Davison[81], E. Dawe[91], I. Dawson[141], K. De[8], R. de Asmundis[106a], A. De Benedetti[115], S. De Castro[22a,22b], S. De Cecco[83], N. De Groot[108], P. de Jong[109], H. De la Torre[93], F. De Lorenzi[67], A. De Maria[57], D. De Pedis[134a], A. De Salvo[134a], U. De Sanctis[151], A. De Santo[151], J.B. De Vivie De Regie[119], W.J. Dearnaley[75], R. Debbe[27], C. Debenedetti[139], D.V. Dedovich[68], N. Dehghanian[3], I. Deigaard[109], M. Del Gaudio[40a,40b], J. Del Peso[85], T. Del Prete[126a,126b], D. Delgove[119], F. Deliot[138], C.M. Delitzsch[52], A. Dell'Acqua[32], L. Dell'Asta[24], M. Dell'Orso[126a,126b], M. Della Pietra[106a,106b], D. della Volpe[52], M. Delmastro[5], P.A. Delsart[58], D.A. DeMarco[161], S. Demers[179], M. Demichev[68], A. Demilly[83], S.P. Denisov[132], D. Denysiuk[138], D. Derendarz[42], J.E. Derkaoui[137d], F. Derue[83], P. Dervan[77], K. Desch[23], C. Deterre[45], K. Dette[46], P.O. Deviveiros[32], A. Dewhurst[133], S. Dhaliwal[25], A. Di Ciaccio[135a,135b], L. Di Ciaccio[5], W.K. Di Clemente[124], C. Di Donato[106a,106b], A. Di Girolamo[32], B. Di Girolamo[32], B. Di Micco[136a,136b], R. Di Nardo[32], K.F. Di Petrillo[59], A. Di Simone[51], R. Di Sipio[161], D. Di Valentino[31], C. Diaconu[88], M. Diamond[161], F.A. Dias[49], M.A. Diaz[34a], E.B. Diehl[92], J. Dietrich[17], S. Díez Cornell[45], A. Dimitrievska[14], J. Dingfelder[23], P. Dita[28b], S. Dita[28b], F. Dittus[32], F. Djama[88], T. Djobava[54b], J.I. Djuvsland[60a], M.A.B. do Vale[26c], D. Dobos[32], M. Dobre[28b], C. Doglioni[84], J. Dolejsi[131], Z. Dolezal[131], M. Donadelli[26d], S. Donati[126a,126b], P. Dondero[123a,123b], J. Donini[37], J. Dopke[133], A. Doria[106a], M.T. Dova[74], A.T. Doyle[56], E. Drechsler[57], M. Dris[10], Y. Du[36b], J. Duarte-Campderros[155], E. Duchovni[175], G. Duckeck[102], O.A. Ducu[97,p], D. Duda[109], A. Dudarev[32], A.Chr. Dudder[86], E.M. Duffield[16], L. Duflot[119], M. Dührssen[32], M. Dumancic[175], A.K. Duncan[56], M. Dunford[60a], H. Duran Yildiz[4a], M. Düren[55], A. Durglishvili[54b], D. Duschinger[47], B. Dutta[45], M. Dyndal[45], C. Eckardt[45], K.M. Ecker[103], R.C. Edgar[92], N.C. Edwards[49], T. Eifert[32], G. Eigen[15], K. Einsweiler[16], T. Ekelof[168], M. El Kacimi[137c], V. Ellajosyula[88], M. Ellert[168], S. Elles[5], F. Ellinghaus[178], A.A. Elliot[172], N. Ellis[32], J. Elmsheuser[27], M. Elsing[32], D. Emeliyanov[133], Y. Enari[157], O.C. Endner[86], J.S. Ennis[173], J. Erdmann[46], A. Ereditato[18], G. Ernis[178], J. Ernst[2], M. Ernst[27], S. Errede[169], E. Ertel[86], M. Escalier[119], H. Esch[46], C. Escobar[127], B. Esposito[50], A.I. Etienvre[138], E. Etzion[155], H. Evans[64], A. Ezhilov[125], F. Fabbri[22a,22b], L. Fabbri[22a,22b], G. Facini[33], R.M. Fakhrutdinov[132], S. Falciano[134a], R.J. Falla[81], J. Faltova[32], Y. Fang[35a], M. Fanti[94a,94b], A. Farbin[8], A. Farilla[136a], C. Farina[127], E.M. Farina[123a,123b], T. Farooque[13], S. Farrell[16], S.M. Farrington[173], P. Farthouat[32], F. Fassi[137e], P. Fassnacht[32], D. Fassouliotis[9], M. Faucci Giannelli[80], A. Favareto[53a,53b], W.J. Fawcett[122], L. Fayard[119], O.L. Fedin[125,q], W. Fedorko[171], S. Feigl[121], L. Feligioni[88], C. Feng[36b], E.J. Feng[32], H. Feng[92], A.B. Fenyuk[132], L. Feremenga[8], P. Fernandez Martinez[170], S. Fernandez Perez[13], J. Ferrando[45], A. Ferrari[168], P. Ferrari[109], R. Ferrari[123a], D.E. Ferreira de Lima[60b], A. Ferrer[170], D. Ferrere[52], C. Ferretti[92], F. Fiedler[86], A. Filipčič[78], M. Filipuzzi[45], F. Filthaut[108], M. Fincke-Keeler[172], K.D. Finelli[152], M.C.N. Fiolhais[128a,128c,r], L. Fiorini[170], A. Fischer[2], C. Fischer[13], J. Fischer[178], W.C. Fisher[93], N. Flaschel[45], I. Fleck[143], P. Fleischmann[92], G.T. Fletcher[141], R.R.M. Fletcher[124], T. Flick[178], B.M. Flierl[102], L.R. Flores Castillo[62a], M.J. Flowerdew[103], G.T. Forcolin[87], A. Formica[138], A. Forti[87], A.G. Foster[19], D. Fournier[119], H. Fox[75], S. Fracchia[13], P. Francavilla[83], M. Franchini[22a,22b], D. Francis[32], L. Franconi[121], M. Franklin[59], M. Frate[166], M. Fraternali[123a,123b], D. Freeborn[81], S.M. Fressard-Batraneanu[32], F. Friedrich[47], D. Froidevaux[32], J.A. Frost[122], C. Fukunaga[158], E. Fullana Torregrosa[86], T. Fusayasu[104], J. Fuster[170], C. Gabaldon[58], O. Gabizon[154], A. Gabrielli[22a,22b], A. Gabrielli[16], G.P. Gach[41a], S. Gadatsch[32], G. Gagliardi[53a,53b], L.G. Gagnon[97], P. Gagnon[64],

C. Galea[108], B. Galhardo[128a,128c], E.J. Gallas[122], B.J. Gallop[133], P. Gallus[130], G. Galster[39], K.K. Gan[113], S. Ganguly[37], J. Gao[36a], Y. Gao[49], Y.S. Gao[145,g], F.M. Garay Walls[49], C. García[170], J.E. García Navarro[170], M. Garcia-Sciveres[16], R.W. Gardner[33], N. Garelli[145], V. Garonne[121], A. Gascon Bravo[45], K. Gasnikova[45], C. Gatti[50], A. Gaudiello[53a,53b], G. Gaudio[123a], L. Gauthier[97], I.L. Gavrilenko[98], C. Gay[171], G. Gaycken[23], E.N. Gazis[10], Z. Gecse[171], C.N.P. Gee[133], Ch. Geich-Gimbel[23], M. Geisen[86], M.P. Geisler[60a], K. Gellerstedt[148a,148b], C. Gemme[53a], M.H. Genest[58], C. Geng[36a,s], S. Gentile[134a,134b], C. Gentsos[156], S. George[80], D. Gerbaudo[13], A. Gershon[155], S. Ghasemi[143], M. Ghneimat[23], B. Giacobbe[22a], S. Giagu[134a,134b], P. Giannetti[126a,126b], S.M. Gibson[80], M. Gignac[171], M. Gilchriese[16], T.P.S. Gillam[30], D. Gillberg[31], G. Gilles[178], D.M. Gingrich[3,d], N. Giokaris[9,*], M.P. Giordani[167a,167c], F.M. Giorgi[22a], P.F. Giraud[138], P. Giromini[59], D. Giugni[94a], F. Giuli[122], C. Giuliani[103], M. Giulini[60b], B.K. Gjelsten[121], S. Gkaitatzis[156], I. Gkialas[9], E.L. Gkougkousis[139], L.K. Gladilin[101], C. Glasman[85], J. Glatzer[13], P.C.F. Glaysher[49], A. Glazov[45], M. Goblirsch-Kolb[25], J. Godlewski[42], S. Goldfarb[91], T. Golling[52], D. Golubkov[132], A. Gomes[128a,128b,128d], R. Gonçalo[128a], R. Goncalves Gama[26a], J. Goncalves Pinto Firmino Da Costa[138], G. Gonella[51], L. Gonella[19], A. Gongadze[68], S. González de la Hoz[170], S. Gonzalez-Sevilla[52], L. Goossens[32], P.A. Gorbounov[99], H.A. Gordon[27], I. Gorelov[107], B. Gorini[32], E. Gorini[76a,76b], A. Gorišek[78], A.T. Goshaw[48], C. Gössling[46], M.I. Gostkin[68], C.R. Goudet[119], D. Goujdami[137c], A.G. Goussiou[140], N. Govender[147b,t], E. Gozani[154], L. Graber[57], I. Grabowska-Bold[41a], P.O.J. Gradin[58], P. Grafström[22a,22b], J. Gramling[52], E. Gramstad[121], S. Grancagnolo[17], V. Gratchev[125], P.M. Gravila[28e], H.M. Gray[32], E. Graziani[136a], Z.D. Greenwood[82,u], C. Grefe[23], K. Gregersen[81], I.M. Gregor[45], P. Grenier[145], K. Grevtsov[5], J. Griffiths[8], A.A. Grillo[139], K. Grimm[75], S. Grinstein[13,v], Ph. Gris[37], J.-F. Grivaz[119], S. Groh[86], E. Gross[175], J. Grosse-Knetter[57], G.C. Grossi[82], Z.J. Grout[81], L. Guan[92], W. Guan[176], J. Guenther[65], F. Guescini[52], D. Guest[166], O. Gueta[155], B. Gui[113], E. Guido[53a,53b], T. Guillemin[5], S. Guindon[2], U. Gul[56], C. Gumpert[32], J. Guo[36c], W. Guo[92], Y. Guo[36a,s], R. Gupta[43], S. Gupta[122], G. Gustavino[134a,134b], P. Gutierrez[115], N.G. Gutierrez Ortiz[81], C. Gutschow[81], C. Guyot[138], C. Gwenlan[122], C.B. Gwilliam[77], A. Haas[112], C. Haber[16], H.K. Hadavand[8], A. Hadef[88], S. Hageböck[23], M. Hagihara[164], H. Hakobyan[180,*], M. Haleem[45], J. Haley[116], G. Halladjian[93], G.D. Hallewell[88], K. Hamacher[178], P. Hamal[117], K. Hamano[172], A. Hamilton[147a], G.N. Hamity[141], P.G. Hamnett[45], L. Han[36a], S. Han[35a], K. Hanagaki[69,w], K. Hanawa[157], M. Hance[139], B. Haney[124], P. Hanke[60a], R. Hanna[138], J.B. Hansen[39], J.D. Hansen[39], M.C. Hansen[23], P.H. Hansen[39], K. Hara[164], A.S. Hard[176], T. Harenberg[178], F. Hariri[119], S. Harkusha[95], R.D. Harrington[49], P.F. Harrison[173], F. Hartjes[109], N.M. Hartmann[102], M. Hasegawa[70], Y. Hasegawa[142], A. Hasib[115], S. Hassani[138], S. Haug[18], R. Hauser[93], L. Hauswald[47], M. Havranek[129], C.M. Hawkes[19], R.J. Hawkings[32], D. Hayakawa[159], D. Hayden[93], C.P. Hays[122], J.M. Hays[79], H.S. Hayward[77], S.J. Haywood[133], S.J. Head[19], T. Heck[86], V. Hedberg[84], L. Heelan[8], K.K. Heidegger[51], S. Heim[124], T. Heim[16], B. Heinemann[45,x], J.J. Heinrich[102], L. Heinrich[112], C. Heinz[55], J. Hejbal[129], L. Helary[32], S. Hellman[148a,148b], C. Helsens[32], J. Henderson[122], R.C.W. Henderson[75], Y. Heng[176], S. Henkelmann[171], A.M. Henriques Correia[32], S. Henrot-Versille[119], G.H. Herbert[17], H. Herde[25], V. Herget[177], Y. Hernández Jiménez[147c], G. Herten[51], R. Hertenberger[102], L. Hervas[32], G.G. Hesketh[81], N.P. Hessey[163a], J.W. Hetherly[43], E. Higón-Rodriguez[170], E. Hill[172], J.C. Hill[30], K.H. Hiller[45], S.J. Hillier[19], I. Hinchliffe[16], E. Hines[124], M. Hirose[51], D. Hirschbuehl[178], O. Hladik[129], X. Hoad[49], J. Hobbs[150], N. Hod[163a], M.C. Hodgkinson[141], P. Hodgson[141], A. Hoecker[32], M.R. Hoeferkamp[107], F. Hoenig[102], D. Hohn[23], T.R. Holmes[16], M. Homann[46], S. Honda[164], T. Honda[69], T.M. Hong[127], B.H. Hooberman[169], W.H. Hopkins[118], Y. Horii[105], A.J. Horton[144], J-Y. Hostachy[58], S. Hou[153], A. Hoummada[137a], J. Howarth[45], J. Hoya[74], M. Hrabovsky[117], I. Hristova[17], J. Hrivnac[119], T. Hryn'ova[5], A. Hrynevich[96], P.J. Hsu[63], S.-C. Hsu[140], Q. Hu[36a], S. Hu[36c], Y. Huang[45], Z. Hubacek[130], F. Hubaut[88], F. Huegging[23], T.B. Huffman[122], E.W. Hughes[38], G. Hughes[75], M. Huhtinen[32], P. Huo[150], N. Huseynov[68,b], J. Huston[93], J. Huth[59], G. Iacobucci[52], G. Iakovidis[27], I. Ibragimov[143],

L. Iconomidou-Fayard[119], E. Ideal[179], P. Iengo[32], O. Igonkina[109,y], T. Iizawa[174], Y. Ikegami[69], M. Ikeno[69], Y. Ilchenko[11,z], D. Iliadis[156], N. Ilic[145], G. Introzzi[123a,123b], P. Ioannou[9,*], M. Iodice[136a], K. Iordanidou[38], V. Ippolito[59], N. Ishijima[120], M. Ishino[157], M. Ishitsuka[159], C. Issever[122], S. Istin[20a], F. Ito[164], J.M. Iturbe Ponce[87], R. Iuppa[162a,162b], H. Iwasaki[69], J.M. Izen[44], V. Izzo[106a], S. Jabbar[3], B. Jackson[124], P. Jackson[1], V. Jain[2], K.B. Jakobi[86], K. Jakobs[51], S. Jakobsen[32], T. Jakoubek[129], D.O. Jamin[116], D.K. Jana[82], R. Jansky[65], J. Janssen[23], M. Janus[57], P.A. Janus[41a], G. Jarlskog[84], N. Javadov[68,b], T. Javůrek[51], M. Javurkova[51], F. Jeanneau[138], L. Jeanty[16], J. Jejelava[54a,aa], G.-Y. Jeng[152], P. Jenni[51,ab], C. Jeske[173], S. Jézéquel[5], H. Ji[176], J. Jia[150], H. Jiang[67], Y. Jiang[36a], Z. Jiang[145], S. Jiggins[81], J. Jimenez Pena[170], S. Jin[35a], A. Jinaru[28b], O. Jinnouchi[159], H. Jivan[147c], P. Johansson[141], K.A. Johns[7], C.A. Johnson[64], W.J. Johnson[140], K. Jon-And[148a,148b], G. Jones[173], R.W.L. Jones[75], S. Jones[7], T.J. Jones[77], J. Jongmanns[60a], P.M. Jorge[128a,128b], J. Jovicevic[163a], X. Ju[176], A. Juste Rozas[13,v], M.K. Köhler[175], A. Kaczmarska[42], M. Kado[119], H. Kagan[113], M. Kagan[145], S.J. Kahn[88], T. Kaji[174], E. Kajomovitz[48], C.W. Kalderon[122], A. Kaluza[86], S. Kama[43], A. Kamenshchikov[132], N. Kanaya[157], S. Kaneti[30], L. Kanjir[78], V.A. Kantserov[100], J. Kanzaki[69], B. Kaplan[112], L.S. Kaplan[176], A. Kapliy[33], D. Kar[147c], K. Karakostas[10], A. Karamaoun[3], N. Karastathis[10], M.J. Kareem[57], E. Karentzos[10], S.N. Karpov[68], Z.M. Karpova[68], K. Karthik[112], V. Kartvelishvili[75], A.N. Karyukhin[132], K. Kasahara[164], L. Kashif[176], R.D. Kass[113], A. Kastanas[149], Y. Kataoka[157], C. Kato[157], A. Katre[52], J. Katzy[45], K. Kawade[105], K. Kawagoe[73], T. Kawamoto[157], G. Kawamura[57], V.F. Kazanin[111,c], R. Keeler[172], R. Kehoe[43], J.S. Keller[45], J.J. Kempster[80], H. Keoshkerian[161], O. Kepka[129], B.P. Kerševan[78], S. Kersten[178], R.A. Keyes[90], M. Khader[169], F. Khalil-zada[12], A. Khanov[116], A.G. Kharlamov[111,c], T. Kharlamova[111,c], T.J. Khoo[52], V. Khovanskiy[99,*], E. Khramov[68], J. Khubua[54b,ac], S. Kido[70], C.R. Kilby[80], H.Y. Kim[8], S.H. Kim[164], Y.K. Kim[33], N. Kimura[156], O.M. Kind[17], B.T. King[77], M. King[170], D. Kirchmeier[47], J. Kirk[133], A.E. Kiryunin[103], T. Kishimoto[157], D. Kisielewska[41a], F. Kiss[51], K. Kiuchi[164], O. Kivernyk[138], E. Kladiva[146b], T. Klapdor-Kleingrothaus[51], M.H. Klein[38], M. Klein[77], U. Klein[77], K. Kleinknecht[86], P. Klimek[110], A. Klimentov[27], R. Klingenberg[46], T. Klioutchnikova[32], E.-E. Kluge[60a], P. Kluit[109], S. Kluth[103], J. Knapik[42], E. Kneringer[65], E.B.F.G. Knoops[88], A. Knue[103], A. Kobayashi[157], D. Kobayashi[159], T. Kobayashi[157], M. Kobel[47], M. Kocian[145], P. Kodys[131], T. Koffas[31], E. Koffeman[109], N.M. Köhler[103], T. Koi[145], H. Kolanoski[17], M. Kolb[60b], I. Koletsou[5], A.A. Komar[98,*], Y. Komori[157], T. Kondo[69], N. Kondrashova[36c], K. Köneke[51], A.C. König[108], T. Kono[69,ad], R. Konoplich[112,ae], N. Konstantinidis[81], R. Kopeliansky[64], S. Koperny[41a], A.K. Kopp[51], K. Korcyl[42], K. Kordas[156], A. Korn[81], A.A. Korol[111,c], I. Korolkov[13], E.V. Korolkova[141], O. Kortner[103], S. Kortner[103], T. Kosek[131], V.V. Kostyukhin[23], A. Kotwal[48], A. Koulouris[10], A. Kourkoumeli-Charalampidi[123a,123b], C. Kourkoumelis[9], V. Kouskoura[27], A.B. Kowalewska[42], R. Kowalewski[172], T.Z. Kowalski[41a], C. Kozakai[157], W. Kozanecki[138], A.S. Kozhin[132], V.A. Kramarenko[101], G. Kramberger[78], D. Krasnopevtsev[100], M.W. Krasny[83], A. Krasznahorkay[32], A. Kravchenko[27], M. Kretz[60c], J. Kretzschmar[77], K. Kreutzfeldt[55], P. Krieger[161], K. Krizka[33], K. Kroeninger[46], H. Kroha[103], J. Kroll[124], J. Kroseberg[23], J. Krstic[14], U. Kruchonak[68], H. Krüger[23], N. Krumnack[67], M.C. Kruse[48], M. Kruskal[24], T. Kubota[91], H. Kucuk[81], S. Kuday[4b], J.T. Kuechler[178], S. Kuehn[51], A. Kugel[60c], F. Kuger[177], T. Kuhl[45], V. Kukhtin[68], R. Kukla[138], Y. Kulchitsky[95], S. Kuleshov[34b], M. Kuna[134a,134b], T. Kunigo[71], A. Kupco[129], O. Kuprash[155], H. Kurashige[70], L.L. Kurchaninov[163a], Y.A. Kurochkin[95], M.G. Kurth[44], V. Kus[129], E.S. Kuwertz[172], M. Kuze[159], J. Kvita[117], T. Kwan[172], D. Kyriazopoulos[141], A. La Rosa[103], J.L. La Rosa Navarro[26d], L. La Rotonda[40a,40b], C. Lacasta[170], F. Lacava[134a,134b], J. Lacey[31], H. Lacker[17], D. Lacour[83], E. Ladygin[68], R. Lafaye[5], B. Laforge[83], T. Lagouri[179], S. Lai[57], S. Lammers[64], W. Lampl[7], E. Lançon[138], U. Landgraf[51], M.P.J. Landon[79], M.C. Lanfermann[52], V.S. Lang[60a], J.C. Lange[13], A.J. Lankford[166], F. Lanni[27], K. Lantzsch[23], A. Lanza[123a], A. Lapertosa[53a,53b], S. Laplace[83], C. Lapoire[32], J.F. Laporte[138], T. Lari[94a], F. Lasagni Manghi[22a,22b],

M. Lassnig[32], P. Laurelli[50], W. Lavrijsen[16], A.T. Law[139], P. Laycock[77], T. Lazovich[59], M. Lazzaroni[94a,94b], B. Le[91], O. Le Dortz[83], E. Le Guirriec[88], E.P. Le Quilleuc[138], M. LeBlanc[172], T. LeCompte[6], F. Ledroit-Guillon[58], C.A. Lee[27], S.C. Lee[153], L. Lee[1], B. Lefebvre[90], G. Lefebvre[83], M. Lefebvre[172], F. Legger[102], C. Leggett[16], A. Lehan[77], G. Lehmann Miotto[32], X. Lei[7], W.A. Leight[31], A.G. Leister[179], M.A.L. Leite[26d], R. Leitner[131], D. Lellouch[175], B. Lemmer[57], K.J.C. Leney[81], T. Lenz[23], B. Lenzi[32], R. Leone[7], S. Leone[126a,126b], C. Leonidopoulos[49], S. Leontsinis[10], G. Lerner[151], C. Leroy[97], A.A.J. Lesage[138], C.G. Lester[30], M. Levchenko[125], J. Levêque[5], D. Levin[92], L.J. Levinson[175], M. Levy[19], D. Lewis[79], B. Li[36a,s], C. Li[36a], H. Li[150], L. Li[48], L. Li[36c], Q. Li[35a], S. Li[48], X. Li[87], Y. Li[143], Z. Liang[35a], B. Liberti[135a], A. Liblong[161], P. Lichard[32], K. Lie[169], J. Liebal[23], W. Liebig[15], A. Limosani[152], S.C. Lin[153,af], T.H. Lin[86], B.E. Lindquist[150], A.E. Lionti[52], E. Lipeles[124], A. Lipniacka[15], M. Lisovyi[60b], T.M. Liss[169], A. Lister[171], A.M. Litke[139], B. Liu[153,ag], D. Liu[153], H. Liu[92], H. Liu[27], J. Liu[36b], J.B. Liu[36a], K. Liu[88], L. Liu[169], M. Liu[36a], Y.L. Liu[36a], Y. Liu[36a], M. Livan[123a,123b], A. Lleres[58], J. Llorente Merino[35a], S.L. Lloyd[79], F. Lo Sterzo[153], E.M. Lobodzinska[45], P. Loch[7], F.K. Loebinger[87], K.M. Loew[25], A. Loginov[179,*], T. Lohse[17], K. Lohwasser[45], M. Lokajicek[129], B.A. Long[24], J.D. Long[169], R.E. Long[75], L. Longo[76a,76b], K.A. Looper[113], J.A. Lopez[34b], D. Lopez Mateos[59], B. Lopez Paredes[141], I. Lopez Paz[13], A. Lopez Solis[83], J. Lorenz[102], N. Lorenzo Martinez[64], M. Losada[21], P.J. Lösel[102], X. Lou[35a], A. Lounis[119], J. Love[6], P.A. Love[75], H. Lu[62a], N. Lu[92], H.J. Lubatti[140], C. Luci[134a,134b], A. Lucotte[58], C. Luedtke[51], F. Luehring[64], W. Lukas[65], L. Luminari[134a], O. Lundberg[148a,148b], B. Lund-Jensen[149], P.M. Luzi[83], D. Lynn[27], R. Lysak[129], E. Lytken[84], V. Lyubushkin[68], H. Ma[27], L.L. Ma[36b], Y. Ma[36b], G. Maccarrone[50], A. Macchiolo[103], C.M. Macdonald[141], B. Maček[78], J. Machado Miguens[124,128b], D. Madaffari[88], R. Madar[37], H.J. Maddocks[168], W.F. Mader[47], A. Madsen[45], J. Maeda[70], S. Maeland[15], T. Maeno[27], A. Maevskiy[101], E. Magradze[57], J. Mahlstedt[109], C. Maiani[119], C. Maidantchik[26a], A.A. Maier[103], T. Maier[102], A. Maio[128a,128b,128d], S. Majewski[118], Y. Makida[69], N. Makovec[119], B. Malaescu[83], Pa. Malecki[42], V.P. Maleev[125], F. Malek[58], U. Mallik[66], D. Malon[6], C. Malone[30], S. Maltezos[10], S. Malyukov[32], J. Mamuzic[170], G. Mancini[50], L. Mandelli[94a], I. Mandić[78], J. Maneira[128a,128b], L. Manhaes de Andrade Filho[26b], J. Manjarres Ramos[163b], A. Mann[102], A. Manousos[32], B. Mansoulie[138], J.D. Mansour[35a], R. Mantifel[90], M. Mantoani[57], S. Manzoni[94a,94b], L. Mapelli[32], G. Marceca[29], L. March[52], G. Marchiori[83], M. Marcisovsky[129], M. Marjanovic[14], D.E. Marley[92], F. Marroquim[26a], S.P. Marsden[87], Z. Marshall[16], S. Marti-Garcia[170], B. Martin[93], T.A. Martin[173], V.J. Martin[49], B. Martin dit Latour[15], M. Martinez[13,v], V.I. Martinez Outschoorn[169], S. Martin-Haugh[133], V.S. Martoiu[28b], A.C. Martyniuk[81], A. Marzin[32], L. Masetti[86], T. Mashimo[157], R. Mashinistov[98], J. Masik[87], A.L. Maslennikov[111,c], I. Massa[22a,22b], L. Massa[22a,22b], P. Mastrandrea[5], A. Mastroberardino[40a,40b], T. Masubuchi[157], P. Mättig[178], J. Mattmann[86], J. Maurer[28b], S.J. Maxfield[77], D.A. Maximov[111,c], R. Mazini[153], I. Maznas[156], S.M. Mazza[94a,94b], N.C. Mc Fadden[107], G. Mc Goldrick[161], S.P. Mc Kee[92], A. McCarn[92], R.L. McCarthy[150], T.G. McCarthy[103], L.I. McClymont[81], E.F. McDonald[91], J.A. Mcfayden[81], G. Mchedlidze[57], S.J. McMahon[133], R.A. McPherson[172,o], M. Medinnis[45], S. Meehan[140], S. Mehlhase[102], A. Mehta[77], K. Meier[60a], C. Meineck[102], B. Meirose[44], D. Melini[170,ah], B.R. Mellado Garcia[147c], M. Melo[146a], F. Meloni[18], S.B. Menary[87], L. Meng[77], X.T. Meng[92], A. Mengarelli[22a,22b], S. Menke[103], E. Meoni[165], S. Mergelmeyer[17], P. Mermod[52], L. Merola[106a,106b], C. Meroni[94a], F.S. Merritt[33], A. Messina[134a,134b], J. Metcalfe[6], A.S. Mete[166], C. Meyer[86], C. Meyer[124], J-P. Meyer[138], J. Meyer[109], H. Meyer Zu Theenhausen[60a], F. Miano[151], R.P. Middleton[133], S. Miglioranzi[53a,53b], L. Mijović[49], G. Mikenberg[175], M. Mikestikova[129], M. Mikuž[78], M. Milesi[91], A. Milic[27], D.W. Miller[33], C. Mills[49], A. Milov[175], D.A. Milstead[148a,148b], A.A. Minaenko[132], Y. Minami[157], I.A. Minashvili[68], A.I. Mincer[112], B. Mindur[41a], M. Mineev[68], Y. Minegishi[157], Y. Ming[176], L.M. Mir[13], K.P. Mistry[124], T. Mitani[174], J. Mitrevski[102], V.A. Mitsou[170], A. Miucci[18], P.S. Miyagawa[141], A. Mizukami[69], J.U. Mjörnmark[84],

M. Mlynarikova[131], T. Moa[148a,148b], K. Mochizuki[97], P. Mogg[51], S. Mohapatra[38], S. Molander[148a,148b], R. Moles-Valls[23], R. Monden[71], M.C. Mondragon[93], K. Mönig[45], J. Monk[39], E. Monnier[88], A. Montalbano[150], J. Montejo Berlingen[32], F. Monticelli[74], S. Monzani[94a,94b], R.W. Moore[3], N. Morange[119], D. Moreno[21], M. Moreno Llácer[57], P. Morettini[53a], S. Morgenstern[32], D. Mori[144], T. Mori[157], M. Morii[59], M. Morinaga[157], V. Morisbak[121], S. Moritz[86], A.K. Morley[152], G. Mornacchi[32], J.D. Morris[79], L. Morvaj[150], P. Moschovakos[10], M. Mosidze[54b], H.J. Moss[141], J. Moss[145,ai], K. Motohashi[159], R. Mount[145], E. Mountricha[27], E.J.W. Moyse[89], S. Muanza[88], R.D. Mudd[19], F. Mueller[103], J. Mueller[127], R.S.P. Mueller[102], T. Mueller[30], D. Muenstermann[75], P. Mullen[56], G.A. Mullier[18], F.J. Munoz Sanchez[87], J.A. Murillo Quijada[19], W.J. Murray[173,133], H. Musheghyan[57], M. Muškinja[78], A.G. Myagkov[132,aj], M. Myska[130], B.P. Nachman[16], O. Nackenhorst[52], K. Nagai[122], R. Nagai[69,ad], K. Nagano[69], Y. Nagasaka[61], K. Nagata[164], M. Nagel[51], E. Nagy[88], A.M. Nairz[32], Y. Nakahama[105], K. Nakamura[69], T. Nakamura[157], I. Nakano[114], R.F. Naranjo Garcia[45], R. Narayan[11], D.I. Narrias Villar[60a], I. Naryshkin[125], T. Naumann[45], G. Navarro[21], R. Nayyar[7], H.A. Neal[92], P.Yu. Nechaeva[98], T.J. Neep[87], A. Negri[123a,123b], M. Negrini[22a], S. Nektarijevic[108], C. Nellist[119], A. Nelson[166], S. Nemecek[129], P. Nemethy[112], A.A. Nepomuceno[26a], M. Nessi[32,ak], M.S. Neubauer[169], M. Neumann[178], R.M. Neves[112], P. Nevski[27], P.R. Newman[19], T. Nguyen Manh[97], R.B. Nickerson[122], R. Nicolaidou[138], J. Nielsen[139], V. Nikolaenko[132,aj], I. Nikolic-Audit[83], K. Nikolopoulos[19], J.K. Nilsen[121], P. Nilsson[27], Y. Ninomiya[157], A. Nisati[134a], R. Nisius[103], T. Nobe[157], M. Nomachi[120], I. Nomidis[31], T. Nooney[79], S. Norberg[115], M. Nordberg[32], N. Norjoharuddeen[122], O. Novgorodova[47], S. Nowak[103], M. Nozaki[69], L. Nozka[117], K. Ntekas[166], E. Nurse[81], F. Nuti[91], D.C. O'Neil[144], A.A. O'Rourke[45], V. O'Shea[56], F.G. Oakham[31,d], H. Oberlack[103], T. Obermann[23], J. Ocariz[83], A. Ochi[70], I. Ochoa[38], J.P. Ochoa-Ricoux[34a], S. Oda[73], S. Odaka[69], H. Ogren[64], A. Oh[87], S.H. Oh[48], C.C. Ohm[16], H. Ohman[168], H. Oide[53a,53b], H. Okawa[164], Y. Okumura[157], T. Okuyama[69], A. Olariu[28b], L.F. Oleiro Seabra[128a], S.A. Olivares Pino[49], D. Oliveira Damazio[27], A. Olszewski[42], J. Olszowska[42], A. Onofre[128a,128e], K. Onogi[105], P.U.E. Onyisi[11,z], M.J. Oreglia[33], Y. Oren[155], D. Orestano[136a,136b], N. Orlando[62b], R.S. Orr[161], B. Osculati[53a,53b,*], R. Ospanov[87], G. Otero y Garzon[29], H. Otono[73], M. Ouchrif[137d], F. Ould-Saada[121], A. Ouraou[138], K.P. Oussoren[109], Q. Ouyang[35a], M. Owen[56], R.E. Owen[19], V.E. Ozcan[20a], N. Ozturk[8], K. Pachal[144], A. Pacheco Pages[13], L. Pacheco Rodriguez[138], C. Padilla Aranda[13], S. Pagan Griso[16], M. Paganini[179], F. Paige[27], P. Pais[89], K. Pajchel[121], G. Palacino[64], S. Palazzo[40a,40b], S. Palestini[32], M. Palka[41b], D. Pallin[37], E.St. Panagiotopoulou[10], I. Panagoulias[10], C.E. Pandini[83], J.G. Panduro Vazquez[80], P. Pani[148a,148b], S. Panitkin[27], D. Pantea[28b], L. Paolozzi[52], Th.D. Papadopoulou[10], K. Papageorgiou[9], A. Paramonov[6], D. Paredes Hernandez[179], A.J. Parker[75], M.A. Parker[30], K.A. Parker[141], F. Parodi[53a,53b], J.A. Parsons[38], U. Parzefall[51], V.R. Pascuzzi[161], E. Pasqualucci[134a], S. Passaggio[53a], Fr. Pastore[80], G. Pásztor[31,al], S. Pataraia[178], J.R. Pater[87], T. Pauly[32], J. Pearce[172], B. Pearson[115], L.E. Pedersen[39], S. Pedraza Lopez[170], R. Pedro[128a,128b], S.V. Peleganchuk[111,c], O. Penc[129], C. Peng[35a], H. Peng[36a], J. Penwell[64], B.S. Peralva[26b], M.M. Perego[138], D.V. Perepelitsa[27], E. Perez Codina[163a], L. Perini[94a,94b], H. Pernegger[32], S. Perrella[106a,106b], R. Peschke[45], V.D. Peshekhonov[68], K. Peters[45], R.F.Y. Peters[87], B.A. Petersen[32], T.C. Petersen[39], E. Petit[58], A. Petridis[1], C. Petridou[156], P. Petroff[119], E. Petrolo[134a], M. Petrov[122], F. Petrucci[136a,136b], N.E. Pettersson[89], A. Peyaud[138], R. Pezoa[34b], P.W. Phillips[133], G. Piacquadio[150], E. Pianori[173], A. Picazio[89], E. Piccaro[79], M. Piccinini[22a,22b], M.A. Pickering[122], R. Piegaia[29], J.E. Pilcher[33], A.D. Pilkington[87], A.W.J. Pin[87], M. Pinamonti[167a,167c,am], J.L. Pinfold[3], A. Pingel[39], S. Pires[83], H. Pirumov[45], M. Pitt[175], L. Plazak[146a], M.-A. Pleier[27], V. Pleskot[86], E. Plotnikova[68], D. Pluth[67], R. Poettgen[148a,148b], L. Poggioli[119], D. Pohl[23], G. Polesello[123a], A. Poley[45], A. Policicchio[40a,40b], R. Polifka[161], A. Polini[22a], C.S. Pollard[56], V. Polychronakos[27], K. Pommès[32], L. Pontecorvo[134a], B.G. Pope[93], G.A. Popeneciu[28c], A. Poppleton[32], S. Pospisil[130], K. Potamianos[16], I.N. Potrap[68], C.J. Potter[30], G. Poulard[32], J. Poveda[32], V. Pozdnyakov[68], M.E. Pozo Astigarraga[32],

P. Pralavorio[88], A. Pranko[16], S. Prell[67], D. Price[87], L.E. Price[6], M. Primavera[76a], S. Prince[90], K. Prokofiev[62c], F. Prokoshin[34b], S. Protopopescu[27], J. Proudfoot[6], M. Przybycien[41a], D. Puddu[136a,136b], M. Purohit[27,an], P. Puzo[119], J. Qian[92], G. Qin[56], Y. Qin[87], A. Quadt[57], W.B. Quayle[167a,167b], M. Queitsch-Maitland[45], D. Quilty[56], S. Raddum[121], V. Radeka[27], V. Radescu[122], S.K. Radhakrishnan[150], P. Radloff[118], P. Rados[91], F. Ragusa[94a,94b], G. Rahal[181], J.A. Raine[87], S. Rajagopalan[27], M. Rammensee[32], C. Rangel-Smith[168], M.G. Ratti[94a,94b], D.M. Rauch[45], F. Rauscher[102], S. Rave[86], T. Ravenscroft[56], I. Ravinovich[175], M. Raymond[32], A.L. Read[121], N.P. Readioff[77], M. Reale[76a,76b], D.M. Rebuzzi[123a,123b], A. Redelbach[177], G. Redlinger[27], R. Reece[139], R.G. Reed[147c], K. Reeves[44], L. Rehnisch[17], J. Reichert[124], A. Reiss[86], C. Rembser[32], H. Ren[35a], M. Rescigno[134a], S. Resconi[94a], E.D. Resseguie[124], O.L. Rezanova[111,c], P. Reznicek[131], R. Rezvani[97], R. Richter[103], S. Richter[81], E. Richter-Was[41b], O. Ricken[23], M. Ridel[83], P. Rieck[103], C.J. Riegel[178], J. Rieger[57], O. Rifki[115], M. Rijssenbeek[150], A. Rimoldi[123a,123b], M. Rimoldi[18], L. Rinaldi[22a], B. Ristić[52], E. Ritsch[32], I. Riu[13], F. Rizatdinova[116], E. Rizvi[79], C. Rizzi[13], R.T. Roberts[87], S.H. Robertson[90,o], A. Robichaud-Veronneau[90], D. Robinson[30], J.E.M. Robinson[45], A. Robson[56], C. Roda[126a,126b], Y. Rodina[88,ao], A. Rodriguez Perez[13], D. Rodriguez Rodriguez[170], S. Roe[32], C.S. Rogan[59], O. Røhne[121], J. Roloff[59], A. Romaniouk[100], M. Romano[22a,22b], S.M. Romano Saez[37], E. Romero Adam[170], N. Rompotis[140], M. Ronzani[51], L. Roos[83], E. Ros[170], S. Rosati[134a], K. Rosbach[51], P. Rose[139], N.-A. Rosien[57], V. Rossetti[148a,148b], E. Rossi[106a,106b], L.P. Rossi[53a], J.H.N. Rosten[30], R. Rosten[140], M. Rotaru[28b], I. Roth[175], J. Rothberg[140], D. Rousseau[119], A. Rozanov[88], Y. Rozen[154], X. Ruan[147c], F. Rubbo[145], M.S. Rudolph[161], F. Rühr[51], A. Ruiz-Martinez[31], Z. Rurikova[51], N.A. Rusakovich[68], A. Ruschke[102], H.L. Russell[140], J.P. Rutherfoord[7], N. Ruthmann[32], Y.F. Ryabov[125], M. Rybar[169], G. Rybkin[119], S. Ryu[6], A. Ryzhov[132], G.F. Rzehorz[57], A.F. Saavedra[152], G. Sabato[109], S. Sacerdoti[29], H.F-W. Sadrozinski[139], R. Sadykov[68], F. Safai Tehrani[134a], P. Saha[110], M. Sahinsoy[60a], M. Saimpert[138], T. Saito[157], H. Sakamoto[157], Y. Sakurai[174], G. Salamanna[136a,136b], A. Salamon[135a,135b], J.E. Salazar Loyola[34b], D. Salek[109], P.H. Sales De Bruin[140], D. Salihagic[103], A. Salnikov[145], J. Salt[170], D. Salvatore[40a,40b], F. Salvatore[151], A. Salvucci[62a,62b,62c], A. Salzburger[32], D. Sammel[51], D. Sampsonidis[156], J. Sánchez[170], V. Sanchez Martinez[170], A. Sanchez Pineda[106a,106b], H. Sandaker[121], R.L. Sandbach[79], M. Sandhoff[178], C. Sandoval[21], D.P.C. Sankey[133], M. Sannino[53a,53b], A. Sansoni[50], C. Santoni[37], R. Santonico[135a,135b], H. Santos[128a], I. Santoyo Castillo[151], K. Sapp[127], A. Sapronov[68], J.G. Saraiva[128a,128d], B. Sarrazin[23], O. Sasaki[69], K. Sato[164], E. Sauvan[5], G. Savage[80], P. Savard[161,d], N. Savic[103], C. Sawyer[133], L. Sawyer[82,u], J. Saxon[33], C. Sbarra[22a], A. Sbrizzi[22a,22b], T. Scanlon[81], D.A. Scannicchio[166], M. Scarcella[152], V. Scarfone[40a,40b], J. Schaarschmidt[175], P. Schacht[103], B.M. Schachtner[102], D. Schaefer[32], L. Schaefer[124], R. Schaefer[45], J. Schaeffer[86], S. Schaepe[23], S. Schaetzel[60b], U. Schäfer[86], A.C. Schaffer[119], D. Schaile[102], R.D. Schamberger[150], V. Scharf[60a], V.A. Schegelsky[125], D. Scheirich[131], M. Schernau[166], C. Schiavi[53a,53b], S. Schier[139], C. Schillo[51], M. Schioppa[40a,40b], S. Schlenker[32], K.R. Schmidt-Sommerfeld[103], K. Schmieden[32], C. Schmitt[86], S. Schmitt[45], S. Schmitz[86], B. Schneider[163a], U. Schnoor[51], L. Schoeffel[138], A. Schoening[60b], B.D. Schoenrock[93], E. Schopf[23], M. Schott[86], J.F.P. Schouwenberg[108], J. Schovancova[8], S. Schramm[52], M. Schreyer[177], N. Schuh[86], A. Schulte[86], M.J. Schultens[23], H.-C. Schultz-Coulon[60a], H. Schulz[17], M. Schumacher[51], B.A. Schumm[139], Ph. Schune[138], A. Schwartzman[145], T.A. Schwarz[92], H. Schweiger[87], Ph. Schwemling[138], R. Schwienhorst[93], J. Schwindling[138], T. Schwindt[23], G. Sciolla[25], F. Scuri[126a,126b], F. Scutti[91], J. Searcy[92], P. Seema[23], S.C. Seidel[107], A. Seiden[139], F. Seifert[130], J.M. Seixas[26a], G. Sekhniaidze[106a], K. Sekhon[92], S.J. Sekula[43], N. Semprini-Cesari[22a,22b], C. Serfon[121], L. Serin[119], L. Serkin[167a,167b], M. Sessa[136a,136b], R. Seuster[172], H. Severini[115], T. Sfiligoj[78], F. Sforza[32], A. Sfyrla[52], E. Shabalina[57], N.W. Shaikh[148a,148b], L.Y. Shan[35a], R. Shang[169], J.T. Shank[24], M. Shapiro[16], P.B. Shatalov[99], K. Shaw[167a,167b], S.M. Shaw[87], A. Shcherbakova[148a,148b], C.Y. Shehu[151], P. Sherwood[81], L. Shi[153,ap], S. Shimizu[70], C.O. Shimmin[166], M. Shimojima[104], S. Shirabe[73], M. Shiyakova[68,aq],

A. Shmeleva[98], D. Shoaleh Saadi[97], M.J. Shochet[33], S. Shojaii[94a], D.R. Shope[115], S. Shrestha[113], E. Shulga[100], M.A. Shupe[7], Z. Si[ag], P. Sicho[129], A.M. Sickles[169], P.E. Sidebo[149], E. Sideras Haddad[147c], O. Sidiropoulou[177], D. Sidorov[116], A. Sidoti[22a,22b], F. Siegert[47], Dj. Sijacki[14], J. Silva[128a,128d], S.B. Silverstein[148a], V. Simak[130], Lj. Simic[14], S. Simion[119], E. Simioni[86], B. Simmons[81], D. Simon[37], M. Simon[86], P. Sinervo[161], N.B. Sinev[118], M. Sioli[22a,22b], G. Siragusa[177], I. Siral[92], S.Yu. Sivoklokov[101], J. Sjölin[148a,148b], M.B. Skinner[75], H.P. Skottowe[59], P. Skubic[115], M. Slater[19], T. Slavicek[130], M. Slawinska[109], K. Sliwa[165], R. Slovak[131], V. Smakhtin[175], B.H. Smart[5], L. Smestad[15], J. Smiesko[146a], S.Yu. Smirnov[100], Y. Smirnov[100], L.N. Smirnova[101,ar], O. Smirnova[84], J.W. Smith[57], M.N.K. Smith[38], R.W. Smith[38], M. Smizanska[75], K. Smolek[130], A.A. Snesarev[98], I.M. Snyder[118], S. Snyder[27], R. Sobie[172,o], F. Socher[47], A. Soffer[155], D.A. Soh[153], G. Sokhrannyi[78], C.A. Solans Sanchez[32], M. Solar[130], E.Yu. Soldatov[100], U. Soldevila[170], A.A. Solodkov[132], A. Soloshenko[68], O.V. Solovyanov[132], V. Solovyev[125], P. Sommer[51], H. Son[165], H.Y. Song[36a,as], A. Sood[16], A. Sopczak[130], V. Sopko[130], V. Sorin[13], D. Sosa[60b], C.L. Sotiropoulou[126a,126b], R. Soualah[167a,167c], A.M. Soukharev[111,c], D. South[45], B.C. Sowden[80], S. Spagnolo[76a,76b], M. Spalla[126a,126b], M. Spangenberg[173], F. Spanò[80], D. Sperlich[17], F. Spettel[103], R. Spighi[22a], G. Spigo[32], L.A. Spiller[91], M. Spousta[131], R.D. St. Denis[56,*], A. Stabile[94a], R. Stamen[60a], S. Stamm[17], E. Stanecka[42], R.W. Stanek[6], C. Stanescu[136a], M. Stanescu-Bellu[45], M.M. Stanitzki[45], S. Stapnes[121], E.A. Starchenko[132], G.H. Stark[33], J. Stark[58], S.H Stark[39], P. Staroba[129], P. Starovoitov[60a], S. Stärz[32], R. Staszewski[42], P. Steinberg[27], B. Stelzer[144], H.J. Stelzer[32], O. Stelzer-Chilton[163a], H. Stenzel[55], G.A. Stewart[56], J.A. Stillings[23], M.C. Stockton[90], M. Stoebe[90], G. Stoicea[28b], P. Stolte[57], S. Stonjek[103], A.R. Stradling[8], A. Straessner[47], M.E. Stramaglia[18], J. Strandberg[149], S. Strandberg[148a,148b], A. Strandlie[121], M. Strauss[115], P. Strizenec[146b], R. Ströhmer[177], D.M. Strom[118], R. Stroynowski[43], A. Strubig[108], S.A. Stucci[27], B. Stugu[15], N.A. Styles[45], D. Su[145], J. Su[127], S. Suchek[60a], Y. Sugaya[120], M. Suk[130], V.V. Sulin[98], S. Sultansoy[4c], T. Sumida[71], S. Sun[59], X. Sun[3], J.E. Sundermann[51], K. Suruliz[151], C.J.E. Suster[152], M.R. Sutton[151], S. Suzuki[69], M. Svatos[129], M. Swiatlowski[33], S.P. Swift[2], I. Sykora[146a], T. Sykora[131], D. Ta[51], K. Tackmann[45], J. Taenzer[155], A. Taffard[166], R. Tafirout[163a], N. Taiblum[155], H. Takai[27], R. Takashima[72], T. Takeshita[142], Y. Takubo[69], M. Talby[88], A.A. Talyshev[111,c], J. Tanaka[157], M. Tanaka[159], R. Tanaka[119], S. Tanaka[69], R. Tanioka[70], B.B. Tannenwald[113], S. Tapia Araya[34b], S. Tapprogge[86], S. Tarem[154], G.F. Tartarelli[94a], P. Tas[131], M. Tasevsky[129], T. Tashiro[71], E. Tassi[40a,40b], A. Tavares Delgado[128a,128b], Y. Tayalati[137e], A.C. Taylor[107], G.N. Taylor[91], P.T.E. Taylor[91], W. Taylor[163b], F.A. Teischinger[32], P. Teixeira-Dias[80], D. Temple[144], H. Ten Kate[32], P.K. Teng[153], J.J. Teoh[120], F. Tepel[178], S. Terada[69], K. Terashi[157], J. Terron[85], S. Terzo[13], M. Testa[50], R.J. Teuscher[161,o], T. Theveneaux-Pelzer[88], J.P. Thomas[19], J. Thomas-Wilsker[80], P.D. Thompson[19], A.S. Thompson[56], L.A. Thomsen[179], E. Thomson[124], M.J. Tibbetts[16], R.E. Ticse Torres[88], V.O. Tikhomirov[98,at], Yu.A. Tikhonov[111,c], S. Timoshenko[100], P. Tipton[179], S. Tisserant[88], K. Todome[159], T. Todorov[5,*], S. Todorova-Nova[131], J. Tojo[73], S. Tokár[146a], K. Tokushuku[69], E. Tolley[59], L. Tomlinson[87], M. Tomoto[105], L. Tompkins[145,au], K. Toms[107], B. Tong[59], P. Tornambe[51], E. Torrence[118], H. Torres[144], E. Torró Pastor[140], J. Toth[88,av], F. Touchard[88], D.R. Tovey[141], T. Trefzger[177], A. Tricoli[27], I.M. Trigger[163a], S. Trincaz-Duvoid[83], M.F. Tripiana[13], W. Trischuk[161], B. Trocmé[58], A. Trofymov[45], C. Troncon[94a], M. Trottier-McDonald[16], M. Trovatelli[172], L. Truong[167a,167c], M. Trzebinski[42], A. Trzupek[42], J.C-L. Tseng[122], P.V. Tsiareshka[95], G. Tsipolitis[10], N. Tsirintanis[9], S. Tsiskaridze[13], V. Tsiskaridze[51], E.G. Tskhadadze[54a], K.M. Tsui[62a], I.I. Tsukerman[99], V. Tsulaia[16], S. Tsuno[69], D. Tsybychev[150], Y. Tu[62b], A. Tudorache[28b], V. Tudorache[28b], T.T. Tulbure[28a], A.N. Tuna[59], S.A. Tupputi[22a,22b], S. Turchikhin[68], D. Turgeman[175], I. Turk Cakir[4b,aw], R. Turra[94a,94b], P.M. Tuts[38], G. Ucchielli[22a,22b], I. Ueda[157], M. Ughetto[148a,148b], F. Ukegawa[164], G. Unal[32], A. Undrus[27], G. Unel[166], F.C. Ungaro[91], Y. Unno[69], C. Unverdorben[102], J. Urban[146b], P. Urquijo[91], P. Urrejola[86], G. Usai[8], J. Usui[69], L. Vacavant[88], V. Vacek[130], B. Vachon[90], C. Valderanis[102],

E. Valdes Santurio[148a,148b], N. Valencic[109], S. Valentinetti[22a,22b], A. Valero[170], L. Valéry[13], S. Valkar[131], J.A. Valls Ferrer[170], W. Van Den Wollenberg[109], P.C. Van Der Deijl[109], H. van der Graaf[109], N. van Eldik[154], P. van Gemmeren[6], J. Van Nieuwkoop[144], I. van Vulpen[109], M.C. van Woerden[109], M. Vanadia[134a,134b], W. Vandelli[32], R. Vanguri[124], A. Vaniachine[160], P. Vankov[109], G. Vardanyan[180], R. Vari[134a], E.W. Varnes[7], T. Varol[43], D. Varouchas[83], A. Vartapetian[8], K.E. Varvell[152], J.G. Vasquez[179], G.A. Vasquez[34b], F. Vazeille[37], T. Vazquez Schroeder[90], J. Veatch[57], V. Veeraraghavan[7], L.M. Veloce[161], F. Veloso[128a,128c], S. Veneziano[134a], A. Ventura[76a,76b], M. Venturi[172], N. Venturi[161], A. Venturini[25], V. Vercesi[123a], M. Verducci[134a,134b], W. Verkerke[109], J.C. Vermeulen[109], A. Vest[47,ax], M.C. Vetterli[144,d], O. Viazlo[84], I. Vichou[169,*], T. Vickey[141], O.E. Vickey Boeriu[141], G.H.A. Viehhauser[122], S. Viel[16], L. Vigani[122], M. Villa[22a,22b], M. Villaplana Perez[94a,94b], E. Vilucchi[50], M.G. Vincter[31], V.B. Vinogradov[68], A. Vishwakarma[45], C. Vittori[22a,22b], I. Vivarelli[151], S. Vlachos[10], M. Vlasak[130], M. Vogel[178], P. Vokac[130], G. Volpi[126a,126b], H. von der Schmitt[103], E. von Toerne[23], V. Vorobel[131], K. Vorobev[100], M. Vos[170], R. Voss[32], J.H. Vossebeld[77], N. Vranjes[14], M. Vranjes Milosavljevic[14], V. Vrba[129], M. Vreeswijk[109], R. Vuillermet[32], I. Vukotic[33], P. Wagner[23], W. Wagner[178], H. Wahlberg[74], S. Wahrmund[47], J. Wakabayashi[105], J. Walder[75], R. Walker[102], W. Walkowiak[143], V. Wallangen[148a,148b], C. Wang[35b], C. Wang[36b,ay], F. Wang[176], H. Wang[16], H. Wang[43], J. Wang[45], J. Wang[152], K. Wang[90], Q. Wang[115], R. Wang[6], S.M. Wang[153], T. Wang[38], W. Wang[36a], C. Wanotayaroj[118], A. Warburton[90], C.P. Ward[30], D.R. Wardrope[81], A. Washbrook[49], P.M. Watkins[19], A.T. Watson[19], M.F. Watson[19], G. Watts[140], S. Watts[87], B.M. Waugh[81], S. Webb[86], M.S. Weber[18], S.W. Weber[177], S.A. Weber[31], J.S. Webster[6], A.R. Weidberg[122], B. Weinert[64], J. Weingarten[57], C. Weiser[51], H. Weits[109], P.S. Wells[32], T. Wenaus[27], T. Wengler[32], S. Wenig[32], N. Wermes[23], M.D. Werner[67], P. Werner[32], M. Wessels[60a], J. Wetter[165], K. Whalen[118], N.L. Whallon[140], A.M. Wharton[75], A. White[8], M.J. White[1], R. White[34b], D. Whiteson[166], F.J. Wickens[133], W. Wiedenmann[176], M. Wielers[133], C. Wiglesworth[39], L.A.M. Wiik-Fuchs[23], A. Wildauer[103], F. Wilk[87], H.G. Wilkens[32], H.H. Williams[124], S. Williams[109], C. Willis[93], S. Willocq[89], J.A. Wilson[19], I. Wingerter-Seez[5], F. Winklmeier[118], O.J. Winston[151], B.T. Winter[23], M. Wittgen[145], M. Wobisch[82,u], T.M.H. Wolf[109], R. Wolff[88], M.W. Wolter[42], H. Wolters[128a,128c], S.D. Worm[133], B.K. Wosiek[42], J. Wotschack[32], M.J. Woudstra[87], K.W. Wozniak[42], M. Wu[58], M. Wu[33], S.L. Wu[176], X. Wu[52], Y. Wu[92], T.R. Wyatt[87], B.M. Wynne[49], S. Xella[39], Z. Xi[92], D. Xu[35a], L. Xu[27], B. Yabsley[152], S. Yacoob[147a], D. Yamaguchi[159], Y. Yamaguchi[120], A. Yamamoto[69], S. Yamamoto[157], T. Yamanaka[157], K. Yamauchi[105], Y. Yamazaki[70], Z. Yan[24], H. Yang[36c], H. Yang[176], Y. Yang[153], Z. Yang[15], W-M. Yao[16], Y.C. Yap[83], Y. Yasu[69], E. Yatsenko[5], K.H. Yau Wong[23], J. Ye[43], S. Ye[27], I. Yeletskikh[68], E. Yildirim[86], K. Yorita[174], R. Yoshida[6], K. Yoshihara[124], C. Young[145], C.J.S. Young[32], S. Youssef[24], D.R. Yu[16], J. Yu[8], J.M. Yu[92], J. Yu[67], L. Yuan[70], S.P.Y. Yuen[23], I. Yusuff[30,az], B. Zabinski[42], G. Zacharis[10], R. Zaidan[66], A.M. Zaitsev[132,aj], N. Zakharchuk[45], J. Zalieckas[15], A. Zaman[150], S. Zambito[59], D. Zanzi[91], C. Zeitnitz[178], M. Zeman[130], A. Zemla[41a], J.C. Zeng[169], Q. Zeng[145], O. Zenin[132], T. Ženiš[146a], D. Zerwas[119], D. Zhang[92], F. Zhang[176], G. Zhang[36a,as], H. Zhang[35b], J. Zhang[6], L. Zhang[51], L. Zhang[36a], M. Zhang[169], R. Zhang[23], R. Zhang[36a,ay], X. Zhang[36b], Y. Zhang[35a], Z. Zhang[119], X. Zhao[43], Y. Zhao[36b,ba], Z. Zhao[36a], A. Zhemchugov[68], J. Zhong[122], B. Zhou[92], C. Zhou[176], L. Zhou[38], L. Zhou[43], M. Zhou[35a], M. Zhou[150], N. Zhou[35c], C.G. Zhu[36b], H. Zhu[35a], J. Zhu[92], Y. Zhu[36a], X. Zhuang[35a], K. Zhukov[98], A. Zibell[177], D. Zieminska[64], N.I. Zimine[68], C. Zimmermann[86], S. Zimmermann[51], Z. Zinonos[57], M. Zinser[86], M. Ziolkowski[143], L. Živković[14], G. Zobernig[176], A. Zoccoli[22a,22b], M. zur Nedden[17], L. Zwalinski[32].

[1] Department of Physics, University of Adelaide, Adelaide, Australia

[2] Physics Department, SUNY Albany, Albany NY, United States of America

[3] Department of Physics, University of Alberta, Edmonton AB, Canada

[4] [(a)] Department of Physics, Ankara University, Ankara; [(b)] Istanbul Aydin University, Istanbul; [(c)]

Division of Physics, TOBB University of Economics and Technology, Ankara, Turkey
[5] LAPP, CNRS/IN2P3 and Université Savoie Mont Blanc, Annecy-le-Vieux, France
[6] High Energy Physics Division, Argonne National Laboratory, Argonne IL, United States of America
[7] Department of Physics, University of Arizona, Tucson AZ, United States of America
[8] Department of Physics, The University of Texas at Arlington, Arlington TX, United States of America
[9] Physics Department, National and Kapodistrian University of Athens, Athens, Greece
[10] Physics Department, National Technical University of Athens, Zografou, Greece
[11] Department of Physics, The University of Texas at Austin, Austin TX, United States of America
[12] Institute of Physics, Azerbaijan Academy of Sciences, Baku, Azerbaijan
[13] Institut de Física d'Altes Energies (IFAE), The Barcelona Institute of Science and Technology, Barcelona, Spain
[14] Institute of Physics, University of Belgrade, Belgrade, Serbia
[15] Department for Physics and Technology, University of Bergen, Bergen, Norway
[16] Physics Division, Lawrence Berkeley National Laboratory and University of California, Berkeley CA, United States of America
[17] Department of Physics, Humboldt University, Berlin, Germany
[18] Albert Einstein Center for Fundamental Physics and Laboratory for High Energy Physics, University of Bern, Bern, Switzerland
[19] School of Physics and Astronomy, University of Birmingham, Birmingham, United Kingdom
[20] [(a)] Department of Physics, Bogazici University, Istanbul; [(b)] Department of Physics Engineering, Gaziantep University, Gaziantep; [(d)] Istanbul Bilgi University, Faculty of Engineering and Natural Sciences, Istanbul,Turkey; [(e)] Bahcesehir University, Faculty of Engineering and Natural Sciences, Istanbul, Turkey, Turkey
[21] Centro de Investigaciones, Universidad Antonio Narino, Bogota, Colombia
[22] [(a)] INFN Sezione di Bologna; [(b)] Dipartimento di Fisica e Astronomia, Università di Bologna, Bologna, Italy
[23] Physikalisches Institut, University of Bonn, Bonn, Germany
[24] Department of Physics, Boston University, Boston MA, United States of America
[25] Department of Physics, Brandeis University, Waltham MA, United States of America
[26] [(a)] Universidade Federal do Rio De Janeiro COPPE/EE/IF, Rio de Janeiro; [(b)] Electrical Circuits Department, Federal University of Juiz de Fora (UFJF), Juiz de Fora; [(c)] Federal University of Sao Joao del Rei (UFSJ), Sao Joao del Rei; [(d)] Instituto de Fisica, Universidade de Sao Paulo, Sao Paulo, Brazil
[27] Physics Department, Brookhaven National Laboratory, Upton NY, United States of America
[28] [(a)] Transilvania University of Brasov, Brasov, Romania; [(b)] Horia Hulubei National Institute of Physics and Nuclear Engineering, Bucharest; [(c)] National Institute for Research and Development of Isotopic and Molecular Technologies, Physics Department, Cluj Napoca; [(d)] University Politehnica Bucharest, Bucharest; [(e)] West University in Timisoara, Timisoara, Romania
[29] Departamento de Física, Universidad de Buenos Aires, Buenos Aires, Argentina
[30] Cavendish Laboratory, University of Cambridge, Cambridge, United Kingdom
[31] Department of Physics, Carleton University, Ottawa ON, Canada
[32] CERN, Geneva, Switzerland
[33] Enrico Fermi Institute, University of Chicago, Chicago IL, United States of America
[34] [(a)] Departamento de Física, Pontificia Universidad Católica de Chile, Santiago; [(b)] Departamento de Física, Universidad Técnica Federico Santa María, Valparaíso, Chile
[35] [(a)] Institute of High Energy Physics, Chinese Academy of Sciences, Beijing; [(b)] Department of Physics, Nanjing University, Jiangsu; [(c)] Physics Department, Tsinghua University, Beijing 100084, China

[36] [(a)] Department of Modern Physics, University of Science and Technology of China, Anhui; [(b)] School of Physics, Shandong University, Shandong; [(c)] Department of Physics and Astronomy, Key Laboratory for Particle Physics, Astrophysics and Cosmology, Ministry of Education; Shanghai Key Laboratory for Particle Physics and Cosmology, Shanghai Jiao Tong University, Shanghai(also at PKU-CHEP);, China
[37] Université Clermont Auvergne, CNRS/IN2P3, LPC, Clermont-Ferrand, France
[38] Nevis Laboratory, Columbia University, Irvington NY, United States of America
[39] Niels Bohr Institute, University of Copenhagen, Kobenhavn, Denmark
[40] [(a)] INFN Gruppo Collegato di Cosenza, Laboratori Nazionali di Frascati; [(b)] Dipartimento di Fisica, Università della Calabria, Rende, Italy
[41] [(a)] AGH University of Science and Technology, Faculty of Physics and Applied Computer Science, Krakow; [(b)] Marian Smoluchowski Institute of Physics, Jagiellonian University, Krakow, Poland
[42] Institute of Nuclear Physics Polish Academy of Sciences, Krakow, Poland
[43] Physics Department, Southern Methodist University, Dallas TX, United States of America
[44] Physics Department, University of Texas at Dallas, Richardson TX, United States of America
[45] DESY, Hamburg and Zeuthen, Germany
[46] Lehrstuhl für Experimentelle Physik IV, Technische Universität Dortmund, Dortmund, Germany
[47] Institut für Kern- und Teilchenphysik, Technische Universität Dresden, Dresden, Germany
[48] Department of Physics, Duke University, Durham NC, United States of America
[49] SUPA - School of Physics and Astronomy, University of Edinburgh, Edinburgh, United Kingdom
[50] INFN Laboratori Nazionali di Frascati, Frascati, Italy
[51] Fakultät für Mathematik und Physik, Albert-Ludwigs-Universität, Freiburg, Germany
[52] Departement de Physique Nucleaire et Corpusculaire, Université de Genève, Geneva, Switzerland
[53] [(a)] INFN Sezione di Genova; [(b)] Dipartimento di Fisica, Università di Genova, Genova, Italy
[54] [(a)] E. Andronikashvili Institute of Physics, Iv. Javakhishvili Tbilisi State University, Tbilisi; [(b)] High Energy Physics Institute, Tbilisi State University, Tbilisi, Georgia
[55] II Physikalisches Institut, Justus-Liebig-Universität Giessen, Giessen, Germany
[56] SUPA - School of Physics and Astronomy, University of Glasgow, Glasgow, United Kingdom
[57] II Physikalisches Institut, Georg-August-Universität, Göttingen, Germany
[58] Laboratoire de Physique Subatomique et de Cosmologie, Université Grenoble-Alpes, CNRS/IN2P3, Grenoble, France
[59] Laboratory for Particle Physics and Cosmology, Harvard University, Cambridge MA, United States of America
[60] [(a)] Kirchhoff-Institut für Physik, Ruprecht-Karls-Universität Heidelberg, Heidelberg; [(b)] Physikalisches Institut, Ruprecht-Karls-Universität Heidelberg, Heidelberg; [(c)] ZITI Institut für technische Informatik, Ruprecht-Karls-Universität Heidelberg, Mannheim, Germany
[61] Faculty of Applied Information Science, Hiroshima Institute of Technology, Hiroshima, Japan
[62] [(a)] Department of Physics, The Chinese University of Hong Kong, Shatin, N.T., Hong Kong; [(b)] Department of Physics, The University of Hong Kong, Hong Kong; [(c)] Department of Physics and Institute for Advanced Study, The Hong Kong University of Science and Technology, Clear Water Bay, Kowloon, Hong Kong, China
[63] Department of Physics, National Tsing Hua University, Taiwan, Taiwan
[64] Department of Physics, Indiana University, Bloomington IN, United States of America
[65] Institut für Astro- und Teilchenphysik, Leopold-Franzens-Universität, Innsbruck, Austria
[66] University of Iowa, Iowa City IA, United States of America
[67] Department of Physics and Astronomy, Iowa State University, Ames IA, United States of America
[68] Joint Institute for Nuclear Research, JINR Dubna, Dubna, Russia
[69] KEK, High Energy Accelerator Research Organization, Tsukuba, Japan

[70] Graduate School of Science, Kobe University, Kobe, Japan
[71] Faculty of Science, Kyoto University, Kyoto, Japan
[72] Kyoto University of Education, Kyoto, Japan
[73] Research Center for Advanced Particle Physics and Department of Physics, Kyushu University, Fukuoka, Japan
[74] Instituto de Física La Plata, Universidad Nacional de La Plata and CONICET, La Plata, Argentina
[75] Physics Department, Lancaster University, Lancaster, United Kingdom
[76] [(a)] INFN Sezione di Lecce; [(b)] Dipartimento di Matematica e Fisica, Università del Salento, Lecce, Italy
[77] Oliver Lodge Laboratory, University of Liverpool, Liverpool, United Kingdom
[78] Department of Experimental Particle Physics, Jožef Stefan Institute and Department of Physics, University of Ljubljana, Ljubljana, Slovenia
[79] School of Physics and Astronomy, Queen Mary University of London, London, United Kingdom
[80] Department of Physics, Royal Holloway University of London, Surrey, United Kingdom
[81] Department of Physics and Astronomy, University College London, London, United Kingdom
[82] Louisiana Tech University, Ruston LA, United States of America
[83] Laboratoire de Physique Nucléaire et de Hautes Energies, UPMC and Université Paris-Diderot and CNRS/IN2P3, Paris, France
[84] Fysiska institutionen, Lunds universitet, Lund, Sweden
[85] Departamento de Fisica Teorica C-15, Universidad Autonoma de Madrid, Madrid, Spain
[86] Institut für Physik, Universität Mainz, Mainz, Germany
[87] School of Physics and Astronomy, University of Manchester, Manchester, United Kingdom
[88] CPPM, Aix-Marseille Université and CNRS/IN2P3, Marseille, France
[89] Department of Physics, University of Massachusetts, Amherst MA, United States of America
[90] Department of Physics, McGill University, Montreal QC, Canada
[91] School of Physics, University of Melbourne, Victoria, Australia
[92] Department of Physics, The University of Michigan, Ann Arbor MI, United States of America
[93] Department of Physics and Astronomy, Michigan State University, East Lansing MI, United States of America
[94] [(a)] INFN Sezione di Milano; [(b)] Dipartimento di Fisica, Università di Milano, Milano, Italy
[95] B.I. Stepanov Institute of Physics, National Academy of Sciences of Belarus, Minsk, Republic of Belarus
[96] Research Institute for Nuclear Problems of Byelorussian State University, Minsk, Republic of Belarus
[97] Group of Particle Physics, University of Montreal, Montreal QC, Canada
[98] P.N. Lebedev Physical Institute of the Russian Academy of Sciences, Moscow, Russia
[99] Institute for Theoretical and Experimental Physics (ITEP), Moscow, Russia
[100] National Research Nuclear University MEPhI, Moscow, Russia
[101] D.V. Skobeltsyn Institute of Nuclear Physics, M.V. Lomonosov Moscow State University, Moscow, Russia
[102] Fakultät für Physik, Ludwig-Maximilians-Universität München, München, Germany
[103] Max-Planck-Institut für Physik (Werner-Heisenberg-Institut), München, Germany
[104] Nagasaki Institute of Applied Science, Nagasaki, Japan
[105] Graduate School of Science and Kobayashi-Maskawa Institute, Nagoya University, Nagoya, Japan
[106] [(a)] INFN Sezione di Napoli; [(b)] Dipartimento di Fisica, Università di Napoli, Napoli, Italy
[107] Department of Physics and Astronomy, University of New Mexico, Albuquerque NM, United States of America
[108] Institute for Mathematics, Astrophysics and Particle Physics, Radboud University Nijmegen/Nikhef,

Nijmegen, Netherlands
[109] Nikhef National Institute for Subatomic Physics and University of Amsterdam, Amsterdam, Netherlands
[110] Department of Physics, Northern Illinois University, DeKalb IL, United States of America
[111] Budker Institute of Nuclear Physics, SB RAS, Novosibirsk, Russia
[112] Department of Physics, New York University, New York NY, United States of America
[113] Ohio State University, Columbus OH, United States of America
[114] Faculty of Science, Okayama University, Okayama, Japan
[115] Homer L. Dodge Department of Physics and Astronomy, University of Oklahoma, Norman OK, United States of America
[116] Department of Physics, Oklahoma State University, Stillwater OK, United States of America
[117] Palacký University, RCPTM, Olomouc, Czech Republic
[118] Center for High Energy Physics, University of Oregon, Eugene OR, United States of America
[119] LAL, Univ. Paris-Sud, CNRS/IN2P3, Université Paris-Saclay, Orsay, France
[120] Graduate School of Science, Osaka University, Osaka, Japan
[121] Department of Physics, University of Oslo, Oslo, Norway
[122] Department of Physics, Oxford University, Oxford, United Kingdom
[123] [(a)] INFN Sezione di Pavia; [(b)] Dipartimento di Fisica, Università di Pavia, Pavia, Italy
[124] Department of Physics, University of Pennsylvania, Philadelphia PA, United States of America
[125] National Research Centre "Kurchatov Institute" B.P.Konstantinov Petersburg Nuclear Physics Institute, St. Petersburg, Russia
[126] [(a)] INFN Sezione di Pisa; [(b)] Dipartimento di Fisica E. Fermi, Università di Pisa, Pisa, Italy
[127] Department of Physics and Astronomy, University of Pittsburgh, Pittsburgh PA, United States of America
[128] [(a)] Laboratório de Instrumentação e Física Experimental de Partículas - LIP, Lisboa; [(b)] Faculdade de Ciências, Universidade de Lisboa, Lisboa; [(c)] Department of Physics, University of Coimbra, Coimbra; [(d)] Centro de Física Nuclear da Universidade de Lisboa, Lisboa; [(e)] Departamento de Fisica, Universidade do Minho, Braga; [(f)] Departamento de Fisica Teorica y del Cosmos and CAFPE, Universidad de Granada, Granada (Spain); [(g)] Dep Fisica and CEFITEC of Faculdade de Ciencias e Tecnologia, Universidade Nova de Lisboa, Caparica, Portugal
[129] Institute of Physics, Academy of Sciences of the Czech Republic, Praha, Czech Republic
[130] Czech Technical University in Prague, Praha, Czech Republic
[131] Charles University, Faculty of Mathematics and Physics, Prague, Czech Republic
[132] State Research Center Institute for High Energy Physics (Protvino), NRC KI, Russia
[133] Particle Physics Department, Rutherford Appleton Laboratory, Didcot, United Kingdom
[134] [(a)] INFN Sezione di Roma; [(b)] Dipartimento di Fisica, Sapienza Università di Roma, Roma, Italy
[135] [(a)] INFN Sezione di Roma Tor Vergata; [(b)] Dipartimento di Fisica, Università di Roma Tor Vergata, Roma, Italy
[136] [(a)] INFN Sezione di Roma Tre; [(b)] Dipartimento di Matematica e Fisica, Università Roma Tre, Roma, Italy
[137] [(a)] Faculté des Sciences Ain Chock, Réseau Universitaire de Physique des Hautes Energies - Université Hassan II, Casablanca; [(b)] Centre National de l'Energie des Sciences Techniques Nucleaires, Rabat; [(c)] Faculté des Sciences Semlalia, Université Cadi Ayyad, LPHEA-Marrakech; [(d)] Faculté des Sciences, Université Mohamed Premier and LPTPM, Oujda; [(e)] Faculté des sciences, Université Mohammed V, Rabat, Morocco
[138] DSM/IRFU (Institut de Recherches sur les Lois Fondamentales de l'Univers), CEA Saclay (Commissariat à l'Energie Atomique et aux Energies Alternatives), Gif-sur-Yvette, France

[139] Santa Cruz Institute for Particle Physics, University of California Santa Cruz, Santa Cruz CA, United States of America
[140] Department of Physics, University of Washington, Seattle WA, United States of America
[141] Department of Physics and Astronomy, University of Sheffield, Sheffield, United Kingdom
[142] Department of Physics, Shinshu University, Nagano, Japan
[143] Department Physik, Universität Siegen, Siegen, Germany
[144] Department of Physics, Simon Fraser University, Burnaby BC, Canada
[145] SLAC National Accelerator Laboratory, Stanford CA, United States of America
[146] [(a)] Faculty of Mathematics, Physics & Informatics, Comenius University, Bratislava; [(b)] Department of Subnuclear Physics, Institute of Experimental Physics of the Slovak Academy of Sciences, Kosice, Slovak Republic
[147] [(a)] Department of Physics, University of Cape Town, Cape Town; [(b)] Department of Physics, University of Johannesburg, Johannesburg; [(c)] School of Physics, University of the Witwatersrand, Johannesburg, South Africa
[148] [(a)] Department of Physics, Stockholm University; [(b)] The Oskar Klein Centre, Stockholm, Sweden
[149] Physics Department, Royal Institute of Technology, Stockholm, Sweden
[150] Departments of Physics & Astronomy and Chemistry, Stony Brook University, Stony Brook NY, United States of America
[151] Department of Physics and Astronomy, University of Sussex, Brighton, United Kingdom
[152] School of Physics, University of Sydney, Sydney, Australia
[153] Institute of Physics, Academia Sinica, Taipei, Taiwan
[154] Department of Physics, Technion: Israel Institute of Technology, Haifa, Israel
[155] Raymond and Beverly Sackler School of Physics and Astronomy, Tel Aviv University, Tel Aviv, Israel
[156] Department of Physics, Aristotle University of Thessaloniki, Thessaloniki, Greece
[157] International Center for Elementary Particle Physics and Department of Physics, The University of Tokyo, Tokyo, Japan
[158] Graduate School of Science and Technology, Tokyo Metropolitan University, Tokyo, Japan
[159] Department of Physics, Tokyo Institute of Technology, Tokyo, Japan
[160] Tomsk State University, Tomsk, Russia, Russia
[161] Department of Physics, University of Toronto, Toronto ON, Canada
[162] [(a)] INFN-TIFPA; [(b)] University of Trento, Trento, Italy, Italy
[163] [(a)] TRIUMF, Vancouver BC; [(b)] Department of Physics and Astronomy, York University, Toronto ON, Canada
[164] Faculty of Pure and Applied Sciences, and Center for Integrated Research in Fundamental Science and Engineering, University of Tsukuba, Tsukuba, Japan
[165] Department of Physics and Astronomy, Tufts University, Medford MA, United States of America
[166] Department of Physics and Astronomy, University of California Irvine, Irvine CA, United States of America
[167] [(a)] INFN Gruppo Collegato di Udine, Sezione di Trieste, Udine; [(b)] ICTP, Trieste; [(c)] Dipartimento di Chimica, Fisica e Ambiente, Università di Udine, Udine, Italy
[168] Department of Physics and Astronomy, University of Uppsala, Uppsala, Sweden
[169] Department of Physics, University of Illinois, Urbana IL, United States of America
[170] Instituto de Fisica Corpuscular (IFIC) and Departamento de Fisica Atomica, Molecular y Nuclear and Departamento de Ingeniería Electrónica and Instituto de Microelectrónica de Barcelona (IMB-CNM), University of Valencia and CSIC, Valencia, Spain
[171] Department of Physics, University of British Columbia, Vancouver BC, Canada

[172] Department of Physics and Astronomy, University of Victoria, Victoria BC, Canada
[173] Department of Physics, University of Warwick, Coventry, United Kingdom
[174] Waseda University, Tokyo, Japan
[175] Department of Particle Physics, The Weizmann Institute of Science, Rehovot, Israel
[176] Department of Physics, University of Wisconsin, Madison WI, United States of America
[177] Fakultät für Physik und Astronomie, Julius-Maximilians-Universität, Würzburg, Germany
[178] Fakultät für Mathematik und Naturwissenschaften, Fachgruppe Physik, Bergische Universität Wuppertal, Wuppertal, Germany
[179] Department of Physics, Yale University, New Haven CT, United States of America
[180] Yerevan Physics Institute, Yerevan, Armenia
[181] Centre de Calcul de l'Institut National de Physique Nucléaire et de Physique des Particules (IN2P3), Villeurbanne, France
[a] Also at Department of Physics, King's College London, London, United Kingdom
[b] Also at Institute of Physics, Azerbaijan Academy of Sciences, Baku, Azerbaijan
[c] Also at Novosibirsk State University, Novosibirsk, Russia
[d] Also at TRIUMF, Vancouver BC, Canada
[e] Also at Department of Physics & Astronomy, University of Louisville, Louisville, KY, United States of America
[f] Also at Physics Department, An-Najah National University, Nablus, Palestine
[g] Also at Department of Physics, California State University, Fresno CA, United States of America
[h] Also at Department of Physics, University of Fribourg, Fribourg, Switzerland
[i] Associated at Department of Physics, Aachen, Tech. Hochsch., Aachen, Germany
[j] Also at Departament de Fisica de la Universitat Autonoma de Barcelona, Barcelona, Spain
[k] Also at Departamento de Fisica e Astronomia, Faculdade de Ciencias, Universidade do Porto, Portugal
[l] Also at Tomsk State University, Tomsk, Russia, Russia
[m] Also at The Collaborative Innovation Center of Quantum Matter (CICQM), Beijing, China
[n] Also at Universita di Napoli Parthenope, Napoli, Italy
[o] Also at Institute of Particle Physics (IPP), Canada
[p] Also at Horia Hulubei National Institute of Physics and Nuclear Engineering, Bucharest, Romania
[q] Also at Department of Physics, St. Petersburg State Polytechnical University, St. Petersburg, Russia
[r] Also at Borough of Manhattan Community College, City University of New York, New York City, United States of America
[s] Also at Department of Physics, The University of Michigan, Ann Arbor MI, United States of America
[t] Also at Centre for High Performance Computing, CSIR Campus, Rosebank, Cape Town, South Africa
[u] Also at Louisiana Tech University, Ruston LA, United States of America
[v] Also at Institucio Catalana de Recerca i Estudis Avancats, ICREA, Barcelona, Spain
[w] Also at Graduate School of Science, Osaka University, Osaka, Japan
[x] Also at Fakultät für Mathematik und Physik, Albert-Ludwigs-Universität, Freiburg, Germany
[y] Also at Institute for Mathematics, Astrophysics and Particle Physics, Radboud University Nijmegen/Nikhef, Nijmegen, Netherlands
[z] Also at Department of Physics, The University of Texas at Austin, Austin TX, United States of America
[aa] Also at Institute of Theoretical Physics, Ilia State University, Tbilisi, Georgia
[ab] Also at CERN, Geneva, Switzerland
[ac] Also at Georgian Technical University (GTU),Tbilisi, Georgia
[ad] Also at Ochadai Academic Production, Ochanomizu University, Tokyo, Japan
[ae] Also at Manhattan College, New York NY, United States of America
[af] Also at Academia Sinica Grid Computing, Institute of Physics, Academia Sinica, Taipei, Taiwan

[ag] Also at School of Physics, Shandong University, Shandong, China
[ah] Also at Departamento de Fisica Teorica y del Cosmos and CAFPE, Universidad de Granada, Granada (Spain), Portugal
[ai] Also at Department of Physics, California State University, Sacramento CA, United States of America
[aj] Also at Moscow Institute of Physics and Technology State University, Dolgoprudny, Russia
[ak] Also at Departement de Physique Nucleaire et Corpusculaire, Université de Genève, Geneva, Switzerland
[al] Also at Eotvos Lorand University, Budapest, Hungary
[am] Also at International School for Advanced Studies (SISSA), Trieste, Italy
[an] Also at Department of Physics and Astronomy, University of South Carolina, Columbia SC, United States of America
[ao] Also at Institut de Física d'Altes Energies (IFAE), The Barcelona Institute of Science and Technology, Barcelona, Spain
[ap] Also at School of Physics, Sun Yat-sen University, Guangzhou, China
[aq] Also at Institute for Nuclear Research and Nuclear Energy (INRNE) of the Bulgarian Academy of Sciences, Sofia, Bulgaria
[ar] Also at Faculty of Physics, M.V.Lomonosov Moscow State University, Moscow, Russia
[as] Also at Institute of Physics, Academia Sinica, Taipei, Taiwan
[at] Also at National Research Nuclear University MEPhI, Moscow, Russia
[au] Also at Department of Physics, Stanford University, Stanford CA, United States of America
[av] Also at Institute for Particle and Nuclear Physics, Wigner Research Centre for Physics, Budapest, Hungary
[aw] Also at Giresun University, Faculty of Engineering, Turkey
[ax] Also at Flensburg University of Applied Sciences, Flensburg, Germany
[ay] Also at CPPM, Aix-Marseille Université and CNRS/IN2P3, Marseille, France
[az] Also at University of Malaya, Department of Physics, Kuala Lumpur, Malaysia
[ba] Also at LAL, Univ. Paris-Sud, CNRS/IN2P3, Université Paris-Saclay, Orsay, France
* Deceased